IL-13–induced intestinal secretory epithelial cell antigen passages are required for IgE-mediated food-induced anaphylaxis

Taeko K. Noah, PhD,[a,b] Kathryn A. Knoop, PhD,[c] Keely G. McDonald, BSc,[c] Jenny K. Gustafsson, PhD,[c] Lisa Waggoner, MS,[b] Simone Vanoni, PhD,[b] Matthew Batie,[d] Kavisha Arora, PhD,[e] Anjaparavanda P. Naren, PhD,[e] Yui-Hsi Wang, PhD,[b] Nicholas W. Lukacs, PhD,[a] Ariel Munitz, PhD,[f] Michael A. Helmrath, MD,[g] Maxime M. Mahe, PhD,[g] Rodney D. Newberry, MD,[c] and Simon P. Hogan, PhD[a,b]

Ann Arbor, Mich, Cincinnati, Ohio, St Louis, Mo, and Tel Aviv, Israel

GRAPHICAL ABSTRACT

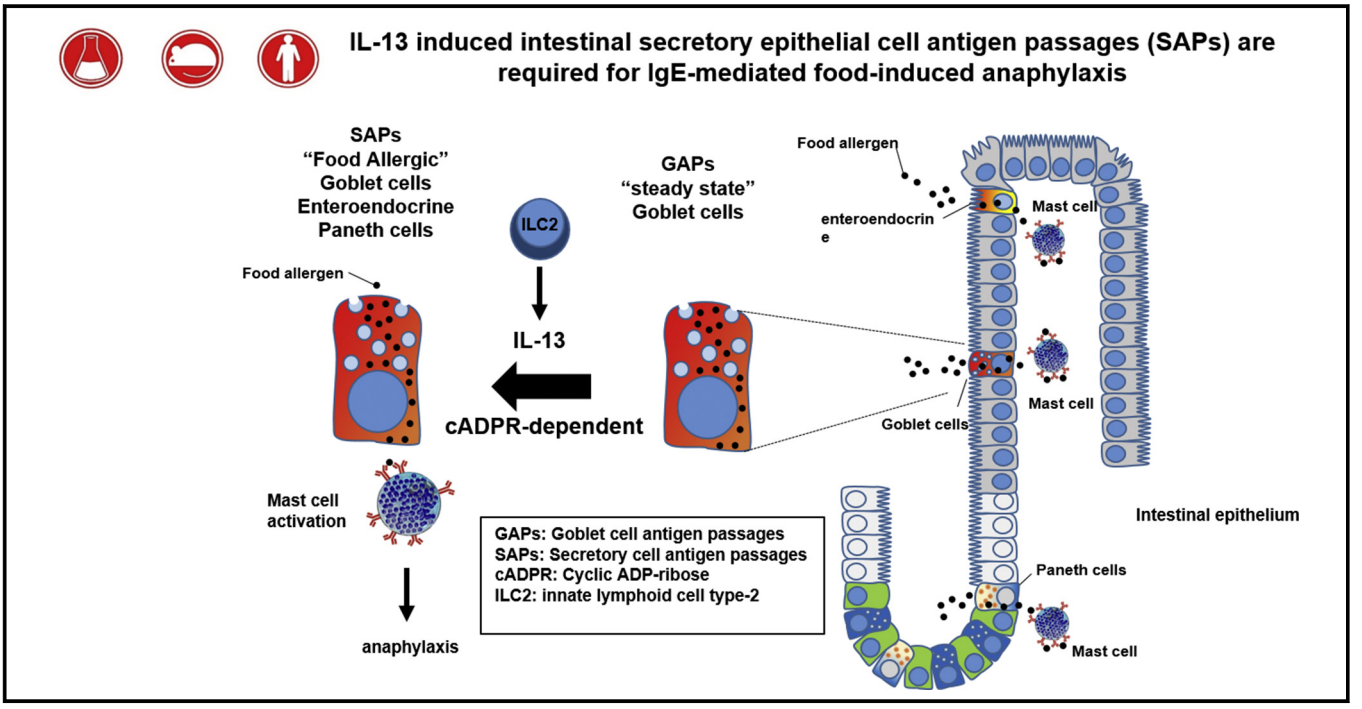

Background: Food-induced anaphylaxis (FIA) is an IgE-dependent immune response that can affect multiple organs and lead to life-threatening complications. The processes by which food allergens cross the mucosal surface and are delivered to the subepithelial immune compartment to promote the clinical manifestations associated with food-triggered anaphylaxis are largely unexplored.

Objective: We sought to define the processes involved in the translocation of food allergens across the mucosal epithelial surface to the subepithelial immune compartment in FIA.
Methods: Two-photon confocal and immunofluorescence microscopy was used to visualize and trace food allergen passage in a murine model of FIA. A human colon cancer cell line, RNA silencing, and pharmacologic approaches were used

From [a]the Mary H. Weiser Food Allergy Center, Department of Pathology, University of Michigan, Ann Arbor; the Divisions of [b]Allergy and Immunology, [g]Pediatric Surgery, [d]Clinical Engineering, and [e]Pulmonary Medicine, Department of Pediatrics, Cincinnati Children's Hospital Medical Center; [c]the Division of Gastroenterology, Washington University School of Medicine St Louis; and [f]the Department of Clinical Microbiology and Immunology, Sackler School of Medicine, Tel Aviv University.

This work was supported by National Institutes of Health grants DK073553, DK090119, AI138177, and AI112626; Food Allergy Research & Education (FARE); Department of Defense grant W81XWH-15-1-051730; M-FARA; and the Mary H. Weiser Food Allergy Center supported (to S.P.H.).

Disclosure of potential conflict of interest: The authors declare that they have no relevant conflicts of interest.

Received for publication August 6, 2018; revised March 15, 2019; accepted for publication April 29, 2019.

Available online June 5, 2019.

Corresponding author: Simon P. Hogan, PhD, Mary H. Weiser Food Allergy Center, Department of Pathology, University of Michigan 4051-BSRB, 109 Zina Pitcher Place, Ann Arbor, MI 48109-2200. E-mail: sihogan@med.umich.edu.

0091-6749/$36.00

https://doi.org/10.1016/j.jaci.2019.04.030

to identify the molecular regulation of intestinal epithelial allergen uptake and translocation. Human intestinal organoid transplants were used to demonstrate the conservation of these molecular processes in human tissues.

Results: Food allergens are sampled by using small intestine (SI) epithelial secretory cells (termed secretory antigen passages [SAPs]) that are localized to the SI villous and crypt region. SAPs channel food allergens to lamina propria mucosal mast cells through an IL-13–CD38–cyclic adenosine diphosphate ribose (cADPR)–dependent process. Blockade of IL-13-induced CD38/cADPR-dependent SAP antigen passaging in mice inhibited induction of clinical manifestations of FIA. IL-13–CD38–cADPR–dependent SAP sampling of food allergens was conserved in human intestinal organoids.

Conclusion: We identify that SAPs are a mechanism by which food allergens are channeled across the SI epithelium mediated by the IL-13/CD38/cADPR pathway, regulate the onset of FIA reactions, and are conserved in human intestine. (J Allergy Clin Immunol 2019;144:1058-73.)

Key words: *Food allergy, antigen passages, intestinal epithelium, mast cells, anaphylaxis, secretory cells*

Anaphylaxis is a severe life-threatening allergic reaction that affects both children and adults and both male and female subjects in the United States.[1] Food avoidance is the primary recommended treatment strategy for food-induced anaphylaxis (FIA), and hospitalization rates for children in the United States have more than doubled from 2000 to 2009.[2]

Clinical and experimental analyses have identified that cross-linking of the food allergen-IgE-FcεR complex on mast cells (MCs) and basophils drives secretion of autacoid mediators that act on target organs (gastrointestinal, cutaneous, respiratory, and cardiovascular organs) and incite the clinical manifestations of FIA.[3-11] Although the immune pathways involved in orchestrating the proallergic inflammatory repertoire and downstream MC effector response have been extensively delineated,[12,13] little is known about how food allergens cross the mucosal barrier and stimulate IgE-MC activation and promotion of the clinical manifestations of disease.

Translocation of oral antigens across the SI epithelium is thought to occur through microfold cell–mediated transcytosis,[14-16] transepithelial dendrites,[17] goblet cell antigen passages (GAPs),[18] and paracellular leak.[19] In healthy subjects microfold cell–mediated transcytosis and GAP-mediated transcellular transport seem to be the primary route of luminal antigen sampling.[18] However, the molecular basis by which food allergens translocate across the allergic intestinal epithelium and induce a food-induced IgE-mediated reaction remains unclear.

Here we demonstrate that secretory epithelial cells in the small intestine (SI) of mice with food allergy act as conduits to permit food allergen transport across the SI epithelium to MCs. We show that SI intestinal secretory epithelial cell antigen passages (secretory antigen passages [SAPs]) that comprise of villi and cryptic goblet cells (GCs), enteroendocrine cells, and Paneth cells; are induced by IL-13 in a CD38/cyclic adenosine diphosphate ribose (cADPR)–dependent manner; and are conserved in human subjects. Our *in vivo* analyses reveal that SAPs are integral for initial translocation of food allergens across the SI epithelium to underlying MCs, which leads to induction of a food-induced anaphylactic reaction.

Abbreviations used

APC:	Allophycocyanin
Atoh1:	Atonal BHLH transcription factor 1
cADPR:	Cyclic adenosine diphosphate ribose
$[Ca^{2+}]_i$:	Intracellular calcium
CCh:	Carbachol
CCHMC:	Cincinnati Children's Medical Center
ChrA:	Chromogranin A
DAPI:	4′,6-Diamidino-2-phenylindole
FIA:	Food-induced anaphylaxis
GAP:	Goblet cell antigen passage
GC:	Goblet cell
HIO:	Human intestinal organoid
ILC2:	Group 2 innate lymphoid cell
IL-4R:	IL-4 receptor
iIL-13Tg:	Intestinal IL-13 transgenic
M4AchR:	Muscarinic type 4 acetylcholine receptor
MC:	Mast cell
MCPT-1:	Mast cell protease 1
MMP7:	Metalloproteinase 7
OVA:	Ovalbumin
PI3K:	Phosphoinositide 3-kinase
Rh-Dex:	Rhodamine-dextran
SAP:	Secretory antigen passage
SI:	Small intestine
STAT6:	Signal transducer and activator of transcription 6
tHIO:	Transplanted human intestinal organoid
WT:	Wild-type

METHODS

Mice

Six- to 10-week old BALB/c (wild-type [WT]), intestinal IL-13–transgenic (iIL-13Tg),[20] and VillinCre^{ERT2} atonal BHLH transcription factor 1 (Atoh1)$^{fl/fl}$ mice[21] were used for GAP/SAP formation analysis and oral antigen–induced anaphylaxis studies.[22] Atoh1^{cre*GR} mice[23] were purchased from the Jackson Laboratory (Stock #013594, Bar Harbor, Me) and crossed to IL-4 receptor (IL-4R) $\alpha^{fl/fl}$ mice[24] and then to IL-9Tg mice.[25] Six- to 10-week old IL-9Tg Atoh1^{cre*PR} IL-4R$\alpha^{fl/fl}$ (IL-4R$\alpha^{\Delta Secretory}$) and IL-9Tg Atoh1^{WT} IL-4R$\alpha^{fl/fl}$ (IL-4Rα^{WT}) mice were used for SAP formation and induction of passive IgE-mediated oral antigen anaphylaxis. Six- to 8-week-old immunodeficient NOD-SCID IL-2Rγ^{null} (NSG) mice obtained from the Comprehensive Mouse and Cancer Core Facility at Cincinnati Children's Medical Center (CCHMC) were used for human intestinal organoid (HIO) transplantation experiments, as previously described.[26] All animals were cared for and handled as described in the protocols approved by the Animal Care and Use Committee at CCHMC and at University of Michigan.

Reagents

Food antigens (cow's milk from the Organic Valley family of farms [La Farge, Wis] and egg from Jay Robb Enterprises [North Palm Beach, Fla], as well as ovalbumin [OVA]) were conjugated to Alexa Fluor 647 dye, as described by the manufacturer (Thermo Fisher Scientific, Waltham, Mass). Model antigens and inhibitors used were as follows: dextran, tetramethylrhodamine, 10,000 MW, lysine fixable and diamidino-2-phenylindole (DAPI; Thermo Fisher Scientific); 8-Br-cADPR (Sigma, St Louis, Mo); tropicamide (Santa Cruz Biotechnology, Dallas, Tex); and LY294002 (Cell Signaling Technology, Danvers, Mass). Reagents used were as follows: Fluo-4 AM and Imject Alum Adjuvant (Thermo Fisher Scientific); RU486, Polybrene, tamoxifen, carbachol (CCh), histamine, and OVA (Sigma-Aldrich, St Louis, Mo); human and mouse IL-13 (PeproTech, Rocky Hill, NJ); mouse anti-IgE antibody; and clone EM-95 (provided by Fred D. Finkelman at CCHMC). Antibodies used were as follows: chromogranin A (ChrA; ImmunoStar,

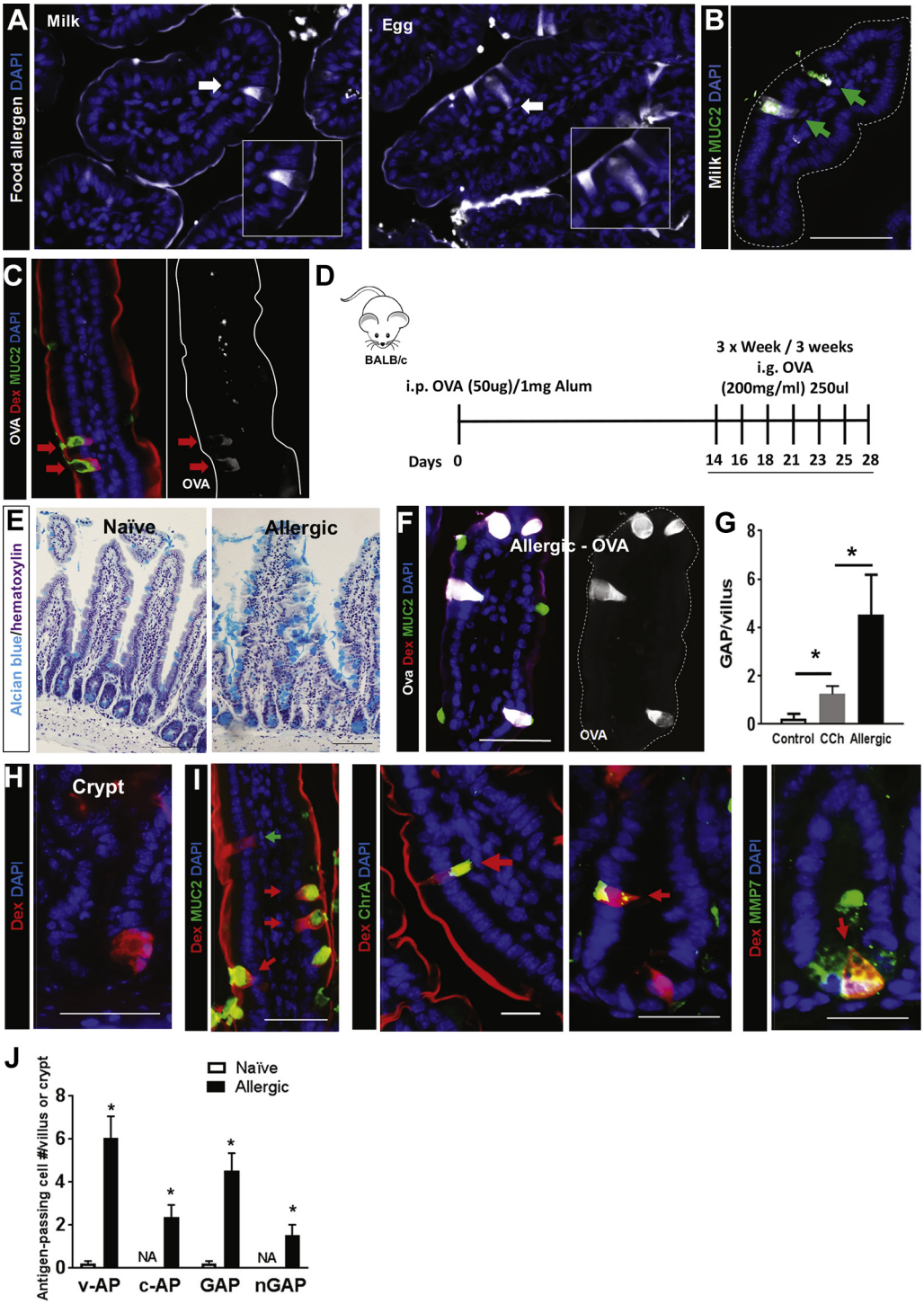

FIG 1. Antigen passage formation was dramatically increased and comprises multiple secretory cell types in allergic mice. **A,** Immunofluorescence analysis of mouse SI villus cross-sections that were exposed to milk or egg conjugated to Alexa Fluor 647 and stimulated with CCh. *White arrows* point to antigen-positive intestinal epithelial cells that are morphologically identified as GCs shown in the *insets*. **B,** Immunofluorescence analysis for MUC2 of mouse SI villus cross-sections that were exposed to milk conjugated to Alexa Fluor 647 and stimulated with CCh. *Green arrows* point to MUC2^{+} GAPs with translocating milk antigens. **C** and **F,** Immunofluorescence analysis of mouse SI from naive mice, CCh-stimulated mice (Fig 1, *C*), and mice with food allergy that are exposed to the food antigen OVA conjugated to Alexa Fluor 647 (Fig 1, *F*, Allergic-OVA). Both types of mice are also exposed to the imaging antigen Rh-Dex *(Dex)* along with the food allergen. The *dotted line* indicates the apical edge of the SI epithelium. **D,** Diagram depicting experimental design for developing food allergy. *i.g.*, Intragastric; *i.p.*, intraperitoneal. **E,** Alcian blue stain with hematoxylin counterstain on SI from naive mice and mice with food allergy to visualize mucin-producing GCs. **G,** GAP quantitation of SI from naive mice (saline-treated control and CCh-treated mice) and

Hudson, Wis); metalloproteinase 7 (MMP7; R&D Systems, Minneapolis, Minn); mouse mast cell protease 1 (MCPT-1; eBioscience, San Diego, Calif); MUC2, signal transducer and activator of transcription 6 (STAT6), IL-4Rα, and phosphorylated STAT6 (Santa Cruz Biotechnology); phosphorylated AKT (Ser473) and phosphorylated AKT (Thr308, #9275; Cell Signaling Technology); actin (A2066; Sigma); DCLK1 and anti–green fluorescent protein (GFP; Abcam, Cambridge, United Kingdom); peridinin-chlorophyll-protein complex–Cy5.5–conjugated CD45R/B220, CD8, Ly-6G/Ly-6C, CD11c, CD3e, phycoerythrin/Cy7–conjugated c-Kit, and biotin-conjugated ST2 (BioLegend, San Diego, Calif); streptavidin-conjugated allophycocyanin (APC)–Cy7 (BD PharMingen, San Jose, Calif); APC-conjugated FcεR (BioLegend); and donkey anti-mouse, anti-rat, anti-rabbit, and anti-goat conjugated to Alexa Fluor 488 or 647 (Invitrogen, Carlsbad, Calif).

Immunofluorescence, histologic analysis, and microscopy

Harvested tissues were fixed in 4% paraformaldehyde in PBS and then processed and embedded either in OCT compound or paraffin. Cross-sections of tissues were stained with the indicated antibodies, and nuclei were visualized with DAPI. All immunofluorescence imaging was performed with a Zeiss Apotome Wide Field Microscope equipped with 10×/0.3 NA, 20×/0.5 NA, 40×/0.75 NA, and 63×/1.4 NA-oil immersion objectives in wide-field mode (Zeiss, Oberkochen, Germany). Z-stack images were reconstructed into 3 dimensions by using Imaris software, and 2-dimensional images were generated by applying extended focus to z-stack images. Photomicrograph images were taken with an Olympus BX51 equipped with a 20×/0.5 NA objective using cellSens software (Olympus, Center Valley, Pa).

Intravital 2-photon microscopy

Imaging of murine gastrointestinal segments was performed, as previously described.[18] Briefly, intact gastrointestinal tissue was surgically extracted from the abdominal cavity and placed on a heated plate mounted on the mouse abdomen to minimize tissue movement caused by mice breathing during imaging. Model fluorescent antigens (rhodamine-dextran [Rh-Dex]) were injected intraluminally 15 minutes before imaging. With naive mice, the SI segment was imaged after PBS exposure.

All imaging was performed with an A1R Multiphoton Upright Confocal Microscope (Nikon, Tokyo, Japan) equipped with a resonant and galvanometric dual scanner was used to take z-stack images. The 25× Apo 1.1 NA LWD water immersion objective was used for imaging. Images were acquired with Nikon NIS elements and then converted to an .avi file format by using Imaris software (Oxford Instruments, Concord, Mass).

In vivo GAP formation analysis with food allergens and immunofluorescence analysis in naive mice and mice with food allergy

Fluorescently tagged clinically relevant food allergens (cow's milk and egg [250 μg/200 μL]), model fluorescent antigens (Rh-Dex), and OVA were intraluminally injected for 20 minutes into naive mouse SI segments. In some experiments, mice were injected with CCh (0.075 mg/kg) before allergen exposure. Naive mice were stimulated with CCh and then exposed to Rh-Dex to examine how oral allergens and imaging antigen translocate across the intestinal epithelium. SI from allergic mice were exposed to OVA (0.45 mg/kg), Rh-Dex (0.0625 g), or both for 20 minutes before tissue harvest. Control mice were injected with saline and then exposed to Rh-Dex (0.0625 g).

Antigen passages were quantitated by counting the frequency of antigen passages in 20 well-oriented villi per mouse for quantitation of GAP formation. Cross-sections of SI from mice with food allergy were stained for MUC2, ChgA, MMP7, or DCLK-1 to determine the cell types translocating Rh-Dex in mice with food allergy on allergen exposure. Villous and crypt antigen-passing intestinal epithelial cells, $MUC2^+$ (GAP) and MUC2− (nGAP) cells in villi are quantified in 20 well-oriented crypts and villi per mouse. OVA and Rh-Dex were intraluminally injected into the stomach, ileum, and colon of mice with food allergy 20 minutes before tissue harvest to assess antigen passages throughout the gastrointestinal tract.

Food allergy was developed in BALB/c WT mice to examine the contribution of intestinal secretory epithelial cell antigen passage (SAP) formation during oral antigen–driven anaphylaxis, as previously described.[22] The symptoms of anaphylaxis were confirmed after the sixth oral antigen challenge, as previously described.[22] Mice with a core body temperature loss of greater than 1.5°C were considered positive for an anaphylactic shock response and used for antigen passage formation analysis experiments. Sixty minutes before the seventh oral antigen challenge, mice with food allergy were treated with inhibitors (either tropicamide [0.1 g in 50 μL volume] or 8-Br-cADPR [0.1 mg/kg 50 μL]) or vehicle (50 μL of saline) for a control group. Core body temperature and signs of diarrhea were monitored over 45 minutes after the oral antigen challenge. Mice were anesthetized, and intact gastrointestinal segments were surgically extracted from the abdominal cavity and intraluminally injected with rhodamine dextran (Rh-Dex) in 2.5 mg/200 μL PBS. SI were harvested 20 minutes after injection and fixed in 4% paraformaldehyde, sucrose protected, and embedded in OCT medium. Eight-micrometer cross-sections were cut and stained for cell markers to identify cell types, and images were captured with a Zeiss Apotome microscope. Antigen passage cell numbers were quantified in at least 20 well-oriented villi per mouse to perform statistical analysis.

In some experiments $Atoh1^{fl/fl}$;*Villin-Cre*^{ERT2} and littermate control ($Atoh1^{fl/fl}$;*Villin-WT*) mice and IL9Tg $Atoh1^{cre*PR}$ IL-4Rα$^{fl/fl}$ and IL9Tg $Atoh1^{WT}$ IL-4Rα$^{fl/fl}$ (WT) mice were intraperitoneally injected with tamoxifen (1 mg per mouse) or RU486 (200 μg per mouse) for 3 consecutive days to drive gene deletion. Mice were intravenously injected with IL-13 (0.025 mg) 4 days after initial tamoxifen or RU486 injection, and SAP formation was examined, as described above. WT BALB/c mice received rmIL-4 (65 ng/200 μL administered intravenously), and 24 hours later, we examined MHC class II expression on splenic $B220^+$ B cells and evidence of SI SAPs to test whether IL-4 is sufficient to drive SAPs, as previously described.[27]

BALB/c mice that had demonstrated evidence of anaphylaxis after the fifth challenge were stratified into either isotype control or anti–IL-13Ra1 mAb treatment groups and received either isotype control mouse IgG_1 (4.5-5.5 g; MOPC-21, mouse IgG_1; BioXCell, Lebanon, NH) or anti-mouse IL-13Rα1 antibody (clone MS8, mouse IgG1-Kappa; 4.5-5.5 g) on days 23, 25, and 27 of the experimental regimen to determine the requirement of IL-13–driven SAPs in the induction of a food-induced anaphylactic reaction. On day 28, mice received the seventh oral OVA challenge, and evidence of a food-induced anaphylactic reaction and SI SAPs was examined.

Antigen localization of MCs in murine food-driven anaphylaxis models

Localization of Rh-Dex to MCs was assessed with immunofluorescence analysis and flow cytometric analysis. For immunofluorescence analyses, SI

allergen-challenged mice with food allergy (n = 3-4 per group). The Student *t* test was used to determine statistical significance, which was indicated with an *asterisk*. **H,** Immunofluorescence cross-section of SI crypts from mice with food allergy. The nucleus was visualized with DAPI (blue). **I,** Immunofluorescence analysis for MUC2, ChrA (an enteroendocrine cell marker), and MMP7 (a Paneth cell marker) was used in allergic mice challenged with OVA and then exposed to Rh-Dex *(Dex)*. **J,** Quantitation of antigen-positive cells, including villus antigen passage *(v-AP)*, crypt antigen passage *(c-AP)*, GAP (villus $MUC2^+$), and nGAP (villus $MUC2^-$) cells in SI from naive mice, saline-treated mice, and allergen-challenged mice with food allergy (n = 3-4 mice per group). *NA*, Zero value.

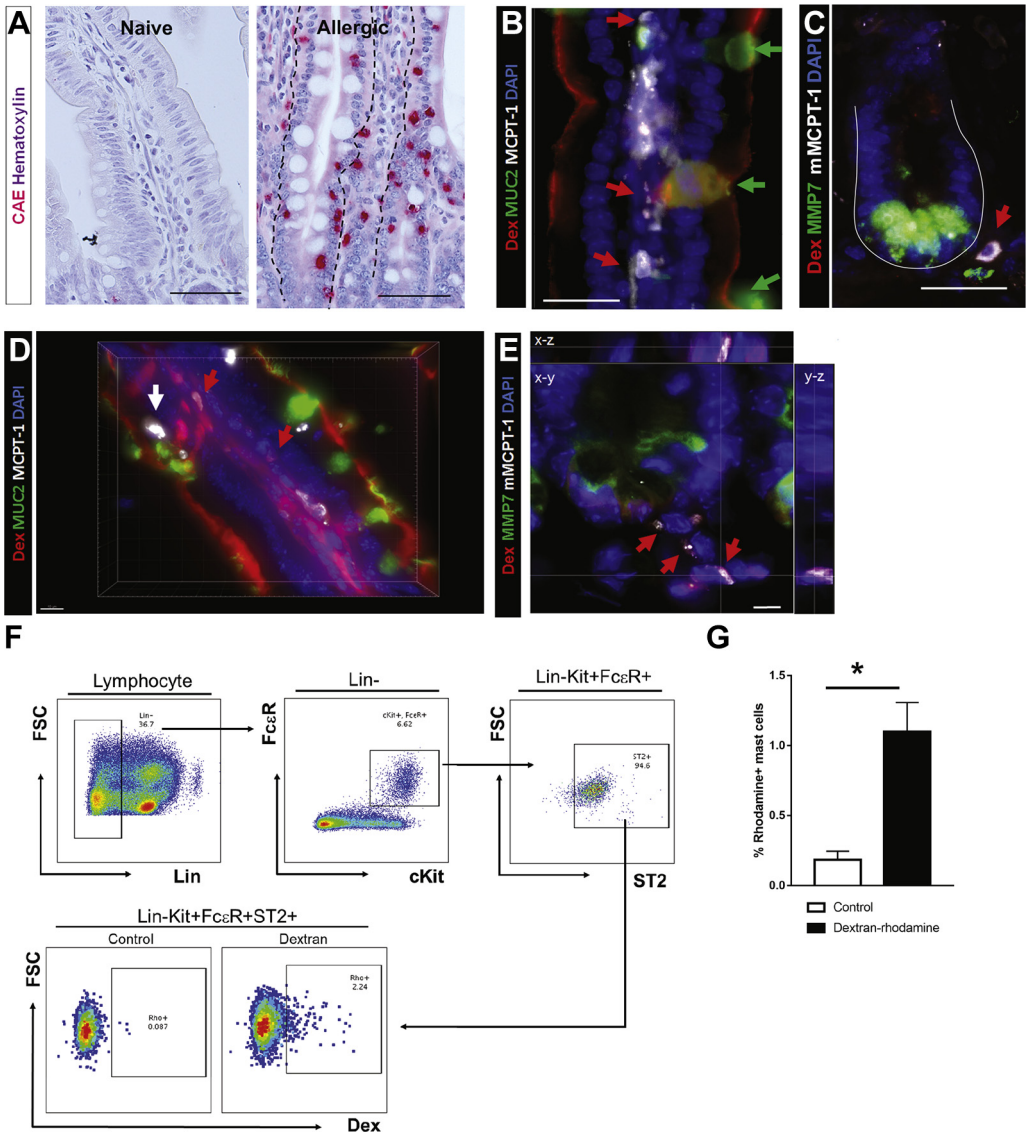

FIG 2. Antigen translocation through SAPs to underlying MCs. **A,** Chloroacetate esterase staining with hematoxylin counterstain on naive mice and allergen-challenged mice with food allergy. The *dotted line* indicates the basal edge of the SI epithelium. **B** and **C,** Immunofluorescence analysis for MUC2 (villus; Fig 2, *B*) or MMP7 (crypt; Fig 2, *C*) of SI from mice with food allergy before food antigen exposure (n = 3-4 mice per group). *Red arrows* point to MCs residing in close proximity to GCs. *Green arrows* point to GCs. The *dotted line* indicates the basal edge of the crypt SI epithelium. **D** and **E,** Three-dimensional reconstruction of immunofluorescence analysis for MUC2 (villus; Fig 2, *D*) or MMP7 (crypt; Fig 2, *E*) of SI from mice with food allergy food antigen exposure (n = 3-4 mice per group). *Red arrows* point to Rh-Dex$^+$ MCs. The *white arrow* points to Rh-Dex$^-$ intraepithelial MCs. **F,** Flow cytometric panels for gating strategies of lamina propria MCs and the level of Rh-Dex in gated MCs (Lin$^-$c-Kit$^+$FcεR$^+$ST2$^+$). *FSC*, Forward scatter. **G,** Flow cytometric analysis of MCs in SI from mice with food allergy for Rh-Dex (n = 8 mice per group). Control mice were exposed to PBS, and Dextran-rhodamine mice were exposed to Rh-Dex along with the food allergen OVA. Data are presented as means ± SEMs. *$P < .05$, Student *t* test or 1-way ANOVA. *Scale bars* = 50 μm for Fig 2, *A*. *Scale bars* = 50, 50, 10, and 5 μm for Fig 2, *B*, *C*, *D*, and *F*, respectively. The nucleus was visualized with DAPI (blue).

segments were stained for anti–MCPT-1 (eBioscience), as described above. MCPT-1$^+$ MCs that colocalize with Rh-Dex were quantified under 5 to 10 high-power fields per mouse and reported as percentage of Rh-Dex$^+$ MCs of total MCs under a high-power field. For flow cytometric analysis, mononuclear cells in the lamina propria were isolated, as previously described,[28] and stained with peridinin-chlorophyll-protein complex–Cy5.5–conjugated antibodies against lineage markers (CD45R/B220, CD8, Ly-6G/Ly-6C, CD11c, and CD3e) and with phycoerythrin/Cy7-conjugated c-Kit and biotin-conjugated ST2 followed by streptavidin-conjugated APC-Cy7 and APC-conjugated FcεR. Stained mononuclear cells were analyzed with a FACSCanto I (BD Biosciences). Quantitation of Rh-Dex$^+$ MCs were performed with FlowJo software (BD Biosciences).

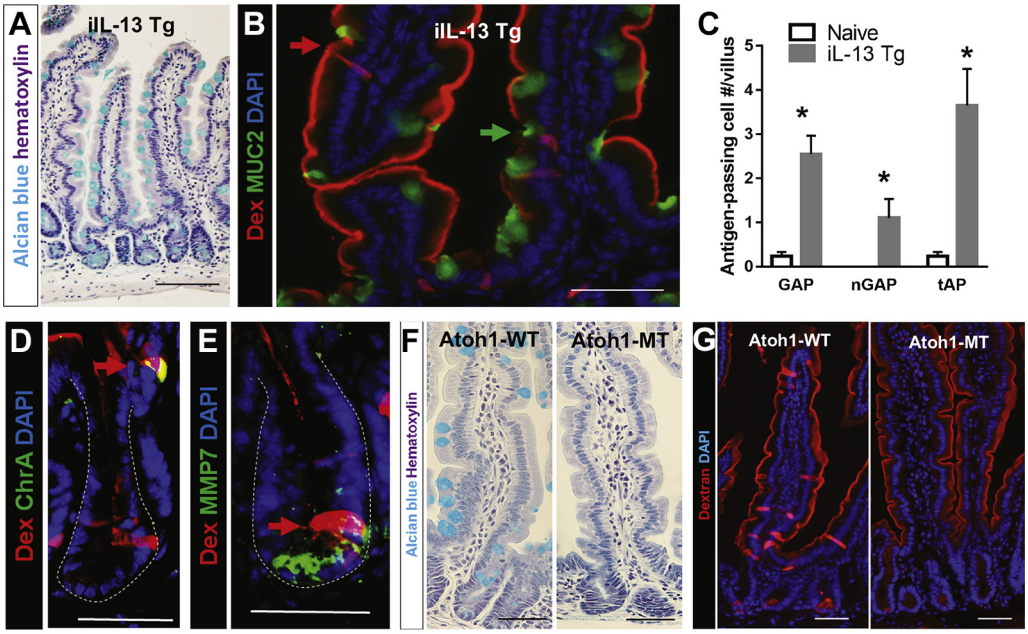

FIG 3. IL-13 is sufficient to drive SAP formation, and secretory cells are required for SAP formation. **A,** Alcian blue stain with hematoxylin counterstain on SI from iIL-13Tg mice to visualize mucin-producing GCs. **B,** Immunofluorescence analysis for MUC2 with SI from iIL-13Tg mice. The *red arrow* points to $MUC2^-$ antigen passage cells, and the *green arrow* points to $MUC2^+$ GAPs. **C,** Quantification of antigen-positive cells in SI from iIL-13Tg and naive control mice (n = 3-4 mice per group). *nGAP*, $MUC2^-$ antigen-positive cells; *tAP*, total antigen passages ($MUC2^+$ and $MUC2^-$). **D** and **E,** Immunofluorescence analysis for ChrA (Fig 3, *D*), an enteroendocrine cell marker, or MMP7 (Fig 4, *E*), a Paneth cell marker, in SI crypts from iIL-13Tg mice. *Dotted lines* indicate basolateral edges of crypts. **F,** Alcian blue stain with hematoxylin counterstain on SI from control (*Atoh1*-WT) and *Atoh1*-deleted (*Atoh1*-MT) mice to visualize mucin-producing GCs. **G,** Immunofluorescence analysis of control (*Atoh1*-WT) and *Atoh1*-deleted (*Atoh1*-MT) SI that were exposed to Rh-Dex. Mice were injected with IL-13 24 hours prior to Rh-Dex exposure. The nucleus was visualized with DAPI. *Scale bars* = 50 μm.

In vitro antigen uptake analysis, immunoblotting, and intracellular calcium measurement

The LS174T cell line was cultured, as previously described.[29] Cells were transduced with recombinant lentivirus carrying short hairpin RNA targeted against human *STAT6* (TRC no. 0000019413) or a nontargeting control along with Polybrene at 10 μg/mL in culture medium for 36 to 48 hours. Transduced cells were exposed to Rh-Dex (0.625 mg/mL PBS) with and without IL-13 (100 ng/mL) for 1 hour. Cells were fixed in 4% paraformaldehyde for 20 minutes and stained for MUC2, and images were captured with the Apotome. Cells were exposed to LY294002 (0, 1, and 10 μmol/L; phosphoinositide 3-kinase [PI3K] inhibitor) or 8-Br-cADPR (0, 5, and 25 μmol/L) for 30 minutes before IL-13 stimulation and exposure to Rh-Dex.

Antigen passage was quantified under a high-power field by using the Zeiss Apotome. Six high-power field images were taken per group to perform statistical analysis.

Western blot analyses were performed, as previously described.[20] In brief, cell lysates harvested from control mice and IL-13 (100 ng/mL) for 30 minutes or 48 hours were loaded in 4–12% Bis-Tris gels and transferred to a nitrocellulose membrane (Invitrogen). Total STAT6, phosphorylated STAT6, total AKT, phosphorylated AKT^{Thr308}, and actin were detected by using antibodies described in the section on "Reagents" and horseradish peroxidase–conjugated secondary antibodies. For intracellular calcium ($[Ca^{2+}]_i$) measurement, LS174T cells were pretreated with 8-Br-cADPR in Krebs buffer for 30 minutes. Cells were loaded with Fluo-4 AM along with IL-13 stimulation for 30 minutes. Fluorescence images of Fluo-4 AM were acquired with an Olympus microscope with a 10× objective. The fluorescent intensity from 6 representative areas was measured and normalized by subtracting an intensity of an area without cells by using Slidebook software. The area under the curve was determined by plotting the fluorescent intensity over 30 minutes with Prism software (GraphPad Software, La Jolla, Calif).

Generation of transplanted HIOs and GAP/SAP analysis

Transplanted human intestinal organoids (tHIOs) were generated and maintained, as previously described.[26] NSG mice carrying tHIOs were treated with IL-13 and inhibitors (tropicamide at 4 mg per mouse in 50 μL of total volume or 8-Br-cADPR at 4 μg per mouse in 50 μL) for 30 minutes to assess GAP/SAP formation in tHIOs. Rh-Dex or Alexa Fluor 647–labeled milk was then injected into the luminal compartment of tHIOs, which was then exposed to GAP/SAP inducers (CCh at 100 μmol/L or IL-13 at 100 ng/mL). tHIOs were fixed in 4% paraformaldehyde for 2 hours at room temperature, sucrose protected overnight, and embedded in OCT. For immunofluorescent analysis, 8-μm-thick sections were used.

Measurement of food allergy parameters

MCPT-1 levels in serum collected after oral allergen challenge were analyzed with an ELISA kit (eBioscience), as described by the manufacturer. SI cross-sections that were embedded in paraffin were stained with Leder stain for chloroacetate esterase activity and Alcian blue. Rectal temperature and hemoconcentration were measured, as previously described.[27]

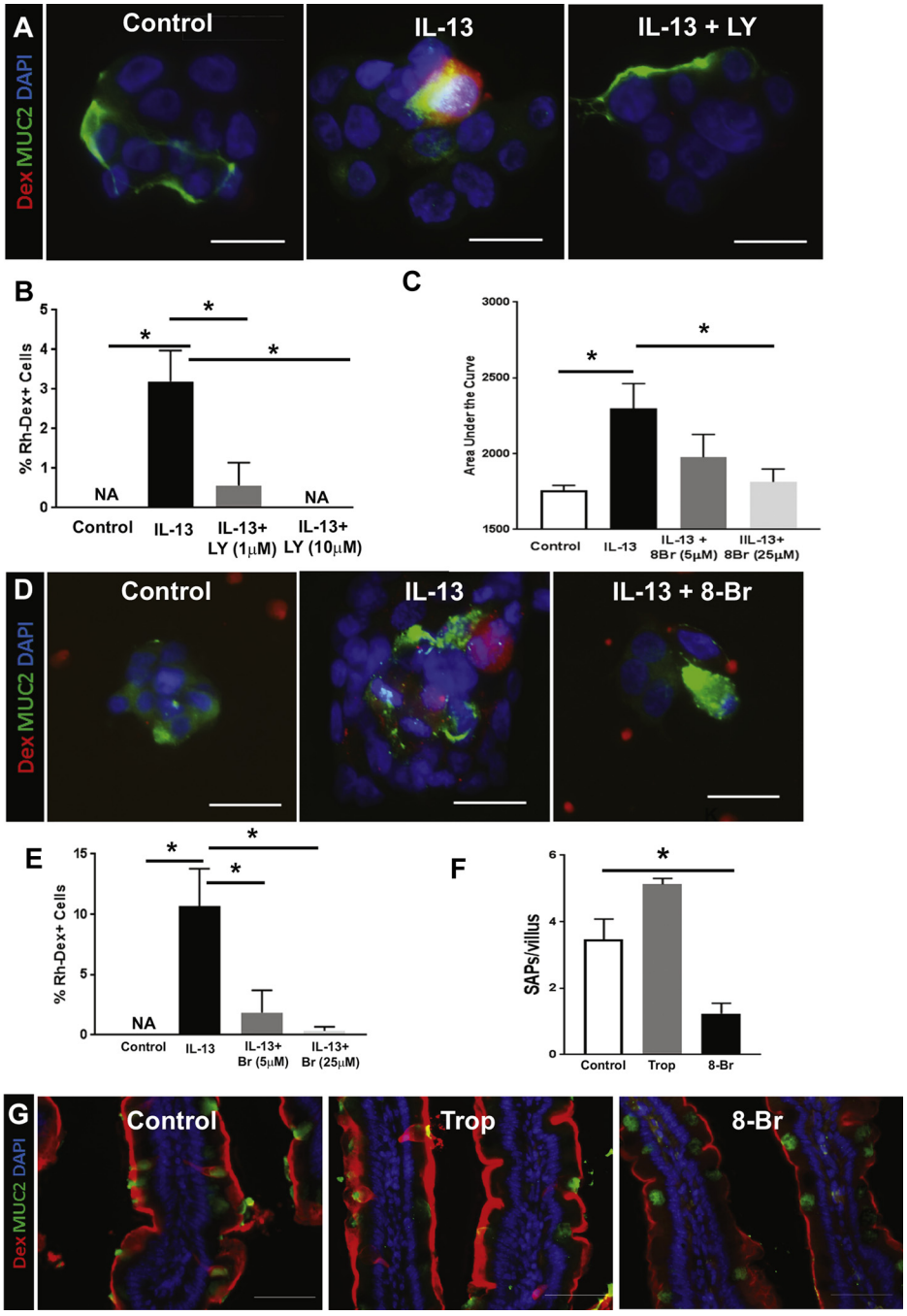

FIG 4. IL-13 drives SAP formation through the PI3K-CD38-cADPR pathway independent of STAT6. **A,** Immunofluorescence analysis for $MUC2^+$ (green) and antigen-positive (red) cells treated with vehicle (control) or PI3K inhibitor (LY294002 *[LY]*) at 10 μmol/L before IL-13 treatment and exposure to Rh-Dex (red). **B,** Quantification of antigen-positive cells per high-power field with cells treated as indicated in Fig 4, *A*. **C,** $[Ca^{2+}]_i$ level measured with Furo-4 AM and quantified as area under the curve over 30 minutes (shown in Fig E2, *F*) in cells treated with vehicle (control), IL-13, or IL-13 and cADPR antagonist (8-Br-cADPR *[8-Br]*). **D,** Immunofluorescence analysis for $MUC2^+$ (green) with cells exposed to Rh-Dex (red) and treated with vehicle (control), IL-13, or IL-13 and 8-Br-cADPR at 25 μmol/L before IL-13 treatment and exposure to Rh-Dex (red). **E,** Quantification of antigen-positive cells per high-power field with cells treated as indicated in Fig 4, *D*. Images and cell counts are representative of 3 independent experiments. **F,** Quantitation of SAP formation per villus of SI from iIL-13Tg mice that are treated with inhibitors as indicated: tropicamide *(Trop)* and 8-Br-cADPR *(8-Br)*. Twenty well-oriented villi were quantified for SAP formation (n = 3-4 mice per group). **G,** Immunofluorescence analysis for SAP formation (red) and the GC marker MUC2 (green) in the SI of iIL-13Tg mice that were treated with inhibitors as indicated: tropicamide *(Trop)* and 8-Br-cADPR *(8-Br)*. In Fig 4, *B*, *C*, *E*, and *F*, data are presented as means ± SEMs. *Scale bars* = 50 μm. The nucleus was visualized with DAPI (blue). **P* < .05, Student *t* test or 1-way ANOVA. *NA*, Zero value.

Statistical analysis

The Student *t* test or 1-way ANOVA and Spearman rank coefficient correlation analysis were performed to determine statistical significance with GraphPad Prism 7 software, unless otherwise noted.

RESULTS

Food allergens translocate across the SI through GCs in villi

Fluorescently labeled food allergens (cow's milk and egg) were intraluminally injected into the SI of naive WT BALB/c mice and monitored for localization by using fluorescence microscopy to examine how food allergens translocate across a mucosal surface. At steady state, we observed a thin layer of food allergen covering the apical surface of the epithelium indicating SI epithelial cell exposure to the allergens (Fig 1, *A*). We observed occasional transepithelial columns (data not shown) that resembled the recently identified CCh-induced GAPs, which act as conduits for the delivery of SI luminal antigens to immune cells.[18]

Fluorescently labeled food allergens were intraluminally administered to naive WT BALB/c mice treated with CCh to determine whether the transepithelial columns were GAPs. We show that the frequency of food allergen–positive SI transepithelial columns were increased after CCh treatment (Fig 1, *A*, white arrows) and localized within MUC2$^+$ cells, indicating that clinically relevant food allergens in naive mice are acquired by GAPs (Fig 1, *B*, green arrows).

Egg antigen OVA is a model food allergen commonly used to induce food-related allergic reactions in mice. To monitor localization of the food allergen OVA and the model imaging protein lysine fixable dextran conjugated with rhodamine (Rh-Dex; 10 kDa) in the SI, we intraluminally coadministered Alexa Fluor 647–labeled OVA and Rh-Dex to naive WT BALB/c mice. Similar to the clinically relevant food allergens, OVA and the imaging protein Rh-Dex localized to MUC2$^+$ transepithelial columns (Fig 1, *C*, red arrows). Colocalization of Rh-Dex and OVA within MUC2$^+$ intestinal epithelial cells in the SI indicates shared SI epithelial uptake processes between clinically relevant food allergens, model food antigens, and model imaging proteins.

Food allergen translocation across SI epithelium is enhanced in mice with food allergy

We next examined food allergen passage in the SI of mice with food allergy. To do this, we developed and used a murine model of food allergy[22] that involves repeated intragastric administration of egg antigen (OVA) to OVA-sensitized BALB/c mice that induces an acute IgE-MC–dependent anaphylactic reaction (Fig 1, *D*),[22,25,30] as evidenced by a hypothermic response within 30 minutes of antigen exposure (see Fig E1, *A*, in this article's Online Repository at www.jacionline.org).

To visualize the spatial and temporal elements of food allergen uptake in the SI of mice with food allergy, we used intravital live imaging with 2-photon microscopy (see Videos E1-E3 in this article's Online Repository at www.jacionline.org). In naive mice the imaging antigen (Rh-Dex) was restricted to the luminal space. We observed occasional transepithelial column formation and SI epithelial antigen uptake (indicated by colocalization of Rh-Dex and DAPI). Furthermore, the lamina propria region beneath DAPI-positive SI epithelium remained free of Rh-Dex (see Video E1). Similarly, examination of the SI of mice with food allergy before allergen exposure revealed infrequent SI transepithelial columns, and the lamina propria was mostly free of Rh-Dex (see Video E2). Exposure of the SI of mice with food allergy to food allergen rapidly enhanced antigen uptake within minutes (see Video E3). Furthermore, we observed accumulation of Rh-Dex within the lamina propria after SI exposure to food allergen, indicating translocation of food allergens across the intestinal epithelium (see Video E3). Immunofluorescence analyses of the SI of BALB/c WT mice with food allergy after food challenge (day 28; Fig 1, *D*) revealed localization of OVA antigen to villus transepithelial columns (Fig 1, *F*). Similarly to naive WT mice, fluorescently labeled OVA and Rh-Dex colocalized to MUC2$^+$ GCs in the SI of mice with food allergy (Fig 1, *C* and *F*). Consistent with live imaging analyses, quantification of the number of GAPs revealed a significantly greater number of antigen passages in the SI of mice with food allergy than those observed in naive WT BALB/c at steady state and after CCh stimulation (Fig 1, *G*). These studies suggest increased luminal antigen uptake in the SI under allergic conditions.

Allergen translocation in the SI of food-allergic mice involves secretory cells in villi and crypts

Repeated intragastric administration of OVA to OVA-sensitized BALB/c mice leads to increased SI GC levels (Alcian blue–positive cells; Fig 1, *E*). Given that GAP formation is tightly associated with GC numbers,[18] we hypothesized that the increase in frequency of OVA$^+$ cells was a consequence of increased numbers of GAPs. Microscopic examination of the SI villus-crypt unit of the allergic mouse indeed revealed increased numbers of antigen-positive GCs (Fig 1, *F* and *J*); however, we also observed the presence of previously undescribed MUC2$^-$Rh-Dex$^+$ cells in the SI villus (Fig 1, *I*, green arrow) and antigen passages within the crypts (Fig 1, *H*). Immunofluorescence analyses of the villus revealed MUC2$^-$Rh-Dex$^+$ cells as enteroendocrine cells (ChrA$^+$), whereas the crypt comprised both enteroendocrine (ChrA$^+$Rh-Dex$^+$) and Paneth (Paneth cell marker MMP7$^+$Rh$^-$Dex$^+$ cells) cells, indicating participation of enteroendocrine and Paneth cells in the uptake of food antigens (Fig 1, *I*, red arrows). The tuft cell marker DCLK1 (see Fig E1, *B*) did not colocalize with Rh-Dex$^+$, indicating that tuft cells do not sample SI food antigens in mice with food allergy. These data indicate that under food allergic conditions, multiple intestinal secretory cell lineages within the SI acquire and channel food antigens from the apical to basolateral side, which we defined as SI intestinal SAPs.

Quantification of Rh-Dex$^+$ cells revealed a greater frequency of villus and the presence of crypt antigen passages in the SI of mice with food allergy, and although GCs were the predominant intestinal secretory cell involved in antigen uptake (approximately 65%), enteroendocrine and Paneth cells can also uptake food allergens (Fig 1, *J*). Examination for SAPs in other gastrointestinal compartments revealed the presence of Rh-Dex$^+$ surface mucous cells within the stomach; however, we observed no Rh-Dex$^+$ staining in the gastric pits within the mucus neck or parietal or chief cells (see Fig E1, *C*). Rh-Dex$^+$ cells were observed within the ileal villus colocalizing with MUC2$^+$ and ChrA$^+$, indicating GCs and enteroendocrine cells forming antigen passages; however, we did not observe evidence of MMP7$^+$ (Paneth) cells forming SAPs at the bottom of the crypts (see Fig E1, *D*). Consistent with our recent findings,[31] we also observed occasional MUC2$^+$ cells

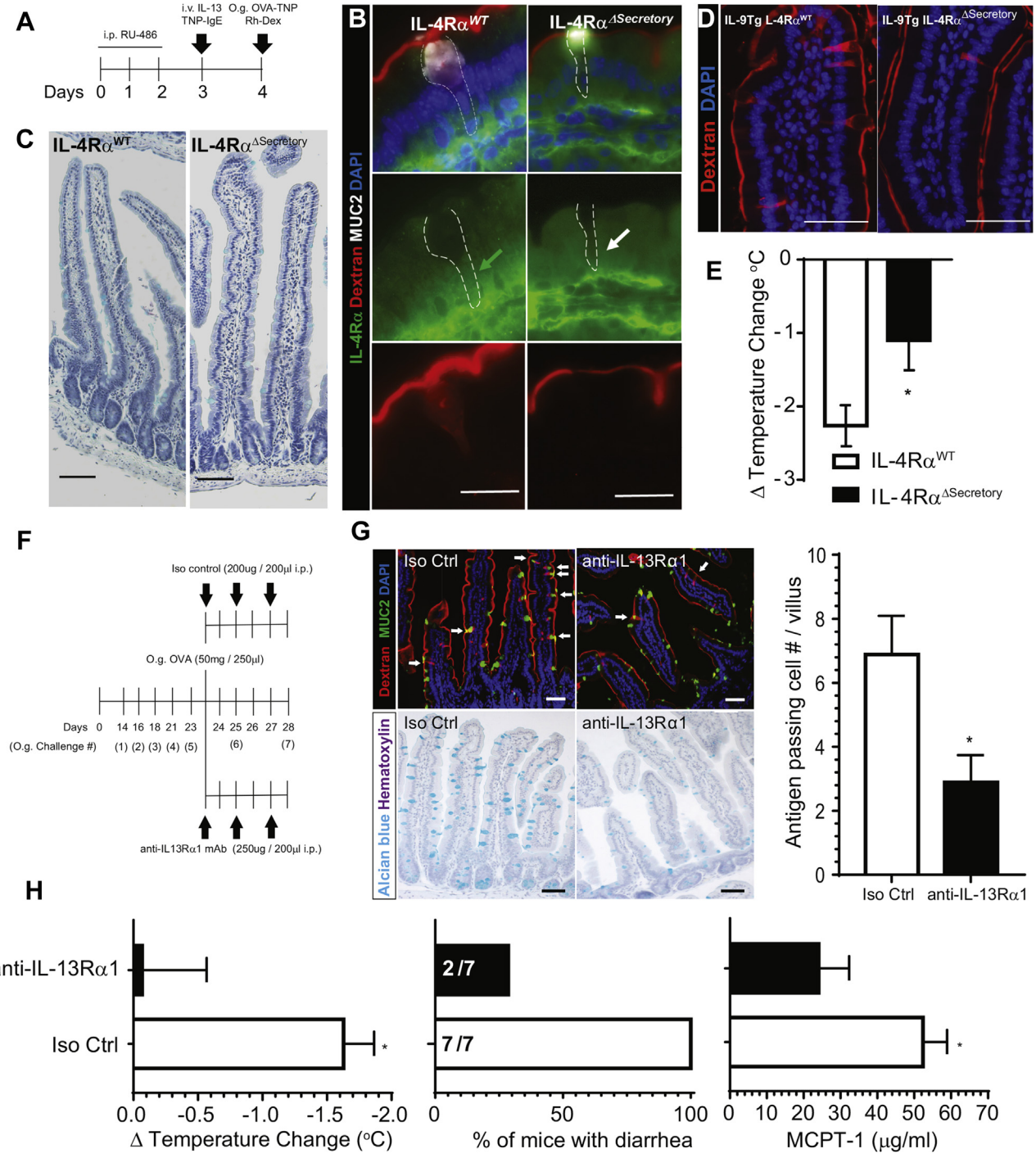

FIG 5. The type II IL-4Rα signaling pathway is required for IL-13-induced SAP formation, luminal allergen translocation, and induction of oral passive IgE and active FIA. **A,** Diagram depicting experimental design for inducible deletion of IL-4Rα in intestinal secretory epithelial cells. **B,** Immunofluorescence analysis for IL-4Rα (green) and MUC2 (white) in mouse SI of IL-4Rα^{WT} and IL-4Rα$^{\Delta secretory}$ mice exposed to Rh-Dex. The *green arrow* depicts the cytoplasm of Rh-Dex^{+}MUC2^{+} GCs in IL-4Rα^{WT} mice that are IL-4Rα^{+}. The *white arrow* depicts cytoplasm of Rh-Dex^{+}MUC2^{+} GCs in IL-4Rα$^{\Delta secretory}$ mice that are IL-4Rα^{-}. The *dotted line* indicates GCs. **C,** Alcian blue staining with hematoxylin counterstain of SI from IL-4Rα^{WT} and IL-4Rα$^{\Delta secretory}$ mice after intraperitoneal RU486. **D,** SI of IL-9Tg IL-4Rα^{WT} and IL-9Tg IL-4Rα$^{\Delta secretory}$ mice treated with RU486 and intraluminal SI challenge of Rh-Dex and OVA-TNP. The nucleus was visualized with DAPI and SAPs by using Rh-Dex^{+} staining. **E,** Δ Temperature (in degrees Celsius at 45 minutes) in IL9Tg IL-4Rα^{WT} and IL-9Tg IL-4Rα$^{\Delta secretory}$ mice treated with RU486, IL-13, and TNP-IgE (described in Fig 5, *A*) after oral TNP-OVA challenge. *$P < .05$. **F,** Experimental regimen for neutralization of IL-13Rα1 using anti–IL-13Rα1 mAb in mice with food allergy. Mice that demonstrated evidence of anaphylaxis (shock) after the fifth oral challenge were stratified into isotype control *(iso control)* or anti–IL-13Rα1 mAb treatment groups.

forming antigen passages within the colon; however, this was rare (see Fig E1, *E*).

Antigen translocation through SAPs to underlying MCs

The onset of FIA in mice requires intestinal mastocytosis and mucosal MC activation mediated by the food antigen–IgE complex.[22,25] From the rapid onset of symptoms of an anaphylactic reaction after allergen consumption (5-10 minutes; see Fig E1, *A*), we hypothesized that SAPs must directly interact with mucosal MCs. Mucosal MCs within the SI of mice with food allergy are predominantly localized to the basolateral membrane of the villous and crypt secretory epithelial cells or within the intraepithelial region positioned midway along the intestinal epithelial cells lateral membrane (Fig 2, *A*, Allergic). Histologic analysis of the SI of mice with food allergy before food antigen exposure (day 28) revealed the presence of mucosal MCPT-1$^+$ MCs in close proximity to villus GCs (Fig 2, *B*, red arrows for MCs and green arrows for GCs) and localized at the basal membrane of crypt Paneth cells (Fig 2, *C*, red arrow). On allergen exposure, we observed enhanced SAP formation, Rh-Dex localization within the lamina propria, and colocalization of Rh-Dex$^+$ and MCPT-1$^+$ MCs in the villi and crypts (Fig 2, *D* and *E*, red arrows, and see Video E6 in this article's Online Repository at www.jacionline.org). SI MC-specific antigen uptake was confirmed by using flow cytometry of SI lamina propria single-cell suspensions, which revealed a significant increase in the number of Rh-Dex$^+$FcεRI$^+$c-Kit$^+$ST2^{high} MCs in mice with food allergy after OVA$^+$ Rh-Dex exposure (Fig 2, *F* and *G*). These studies suggest that SI SAPs rapidly channel food antigens to mucosal MCs in mice with food allergy.

IL-13 is sufficient to drive SAP formation, and secretory cells are required for IL-13–driven antigen passages

The proallergic cytokine IL-13 plays a major role in the induction of the clinical manifestations of FIA[32] and has been shown to modulate intestinal secretory epithelial cell lineage function, including GC hyperplasia (Fig 3, *A*).[20] Thus we hypothesized that IL-13 can stimulate SI SAPs. Indeed, analyses of intestinal iIL-13Tg mice revealed that ectopic expression of IL-13 in the SI epithelium is sufficient to induce SAPs (Fig 3, *B*, green and red arrows). Cross-sectional analysis of SI indicates that GC and GAP abundance was significantly higher in iIL-13Tg than WT (BALB/c) mice (naive mice: 0.40 ± 0.03 vs iIL-13Tg mice: 2.60 ± 0.41; GAPs/villi, $P < .05$; Fig 3, *C*). In addition to the increased GAP formation in iIL-13Tg villi, we identified MUC2$^-$ antigen passages in the SI villi and crypts of iIL-13Tg mice similar to those in mice with food allergy (Fig 3, *B-E*), indicating that SI overexpression of IL-13 is sufficient to mimic the SI SAP phenotype observed in mice with food allergy.

To determine the requirement of SI secretory epithelial cells in SAP formation driven by IL-13, we used *Atoh1* mutant mice (*Atoh1*-MT), in which all cells of the secretory lineage are deleted from the intestinal epithelium after tamoxifen treatment.[33] Treatment of *Atoh1*-MT mice with tamoxifen led to a loss of secretory lineage cells in the SI (Fig 3, *F*). Intraluminal administration of Rh-Dex to *Atoh1*-WT mice treated with IL-13 revealed SAP formation in the villi and crypts (Fig 3, *G*). Tamoxifen treatment alone of *Atoh1*-WT mice did not drive SAP formation (see Fig E1, *F*). In contrast to Atoh1-WT mice, we observed no evidence of SI villus or crypt transepithelial columns in *Atoh1*-MT mice (Fig 3, *G*), indicating that intestinal epithelial cells of the secretory lineage are required for IL-13–driven luminal antigen passage formation.

IL-13 drives SAP formation through a STAT6-independent PI3K–CD38–cADPR–dependent process

To study the signaling cascade involved in IL-13–induced SAP formation, we used LS174T, a mucinous colon cancer cell line.[29] We show that exposure of LS174T cells to IL-13 induced antigen uptake (see Fig E2, *A*, in this article's Online Repository at www.jacionline.org; Rh-Dex$^+$ cells) that was associated with the type II IL-4R–dependent STAT6/PI3K activation, as evidenced by phosphorylation of STAT6 and AKT^{Ser473} (see Fig E2, *B-E*). Genetic abrogation of STAT6 in LS174T cells did not reduce IL-13–mediated antigen uptake, indicating that IL-13 induced SAPs independent of STAT6 signaling (see Fig E2, *A* and *G*). In contrast, pharmacologically inhibiting the PI3K pathway (LY294002, a specific PI3K inhibitor) inhibited IL-13–induced antigen uptake in a dose-dependent manner (IL-13: 0.03 ± 0.01 vs IL-13 + LY294002 [1 μmol/L]: 0.01 ± 0.01 or IL-13 + LY294002 [10 μmol/L]: 0 ± 0.00, percentage Rh-Dex$^+$ cells [mean ± SEM]; $P < .05$; Fig 4, *A* and *B*).

Given that IL-13–induced PI3K activation drives $[Ca^{2+}]_i$ release through a CD38/cADPR-dependent mechanism[34] and that $[Ca^{2+}]_i$ release is strongly associated with secretatogogue activity,[35] we examined the necessity of the CD38/cADPR pathway in IL-13–induced antigen uptake. Inhibiting the CD38/cADPR pathway with the cADPR antagonist 8-Br-cADPR abrogated IL-13–induced $[Ca^{2+}]_i$ release in LS174T cells in a dose-dependent manner (Fig 4, *C*, and see Fig E2, *F*). Abrogation of IL-13–induced $[Ca^{2+}]_i$ in LS174T cells inhibited SAP formation (IL-13: 0.11 ± 0.03 vs 8-Br-cADPR [5 μmol/L]: 0.02 ± 0.02 or 8-Br-cADPR [10 μmol/L]: 0.01 ± 0.01, percentage Rho-Dex$^+$ cells [mean ± SEM]; $P < .05$; Fig 4, *D* and *E*). Consistent with our *in vitro* analyses, treating iIL-13Tg mice with 8-Br-cADPR suppressed SAP formation in the SIs (Fig 4, *F* and *G*). Treating iIL-13Tg mice with the muscarinic type 4 acetylcholine receptor (M4AchR) antagonist tropicamide did not affect the frequency of SAPs (Fig 4, *F* and *G*), indicating that IL-13–driven SAP

Experimental analyses were performed after the seventh oral challenge on day 28. **G,** Immunofluorescence analysis for MUC2 (green) and SAPs (Rh-Dex$^+$): Alcian blue staining with hematoxylin counterstain of SI and quantitation of antigen passing cells per villus/SI from isotype control *(Iso Ctrl)* of SI of control and anti–IL-13Rα1–treated mice. **H,** Δ Temperature (in degrees Celsius) and percentage of mice with diarrhea and serum MCPT-1 levels (at 45 minutes) in isotype control–treated *(Iso Ctrl)* and anti–IL-13Rα1–treated mice after the seventh oral OVA challenge on day 28, as indicated in Fig 5, *F*. Fractions indicate the number of mice with diarrhea of the total number of mice. *Scale bars* = 50 μm (Fig 5, *B*, *D*, *G*, and *H*) and 20 μm (Fig 5, *C*). *i.p.*, Intraperitoneal; *i.v.*, intravenous; *O.g.*, oral gavage. *$P < .05$.

formation is dependent on the CD38/cADPR pathway and independent of the M4AchR pathway. Collectively, these data support that IL-13 induces SAPs through a CD38/cADPR-dependent $[Ca^{2+}]_i$ release mechanism.

IL-13 directly drives antigen passage formation on intestinal secretory cells

To determine the requirement of intestinal epithelial secretory cell IL-13 signaling on SAP formation and FIA, we crossed Atoh1^{Cre*GR}IL4Rα$^{F/F}$ mice to IL9Tg mice in which IL-9 was ectopically expressed in the SI epithelium and promoted mastocytosis in the SI.[25] We show that administration of the competitive progesterone receptor antagonist RU486 deleted IL-4Rα from Atoh1^{+} cell lineages (Fig 5, *A* and *B*, white arrow). Deletion of IL-4Rα from secretory cells did not cause any obvious morphologic changes in SIs at steady state (Fig 5, *C*). Genetic deletion of IL-4Rα from secretory intestinal epithelial cell lineages inhibited IL-13–induced SAP formation (Fig 5, *B* and *D*), indicating involvement of secretory cells in antigen passage formation and dependency on intestinal epithelial IL-13 signaling through IL-4Rα for antigen passage formation. Administration of RU486, anti-TNP IgE, and IL-13 to IL9Tg Atoh1^{WT}IL4Rα$^{F/F}$ mice (IL-4Rα^{WT}; IL9Tg) and subsequent oral challenge with antigen (TNP-OVA) induced a shock response (Fig 5, *E*). In contrast, injection of anti–TNP-IgE and IL-13 and subsequent TNP-OVA challenge of IL-9Tg Atoh11^{Cre*GR}IL4Rα$^{fl/fl}$ mice (IL-4Rα$^{\Delta Secretory}$; IL9Tg) that received RU486 did not have a shock response (Fig 5, *E*). These studies indicate that the intestinal epithelial secretory cell–intrinsic IL-4Rα pathway is required for IL-13–induced SAP formation and induction of passive IgE-mediated oral antigen anaphylaxis.

Blockade of IL-13–IL-13Rα1 signaling reduces antigen passages and protects against food-induced anaphylactic shock

The demonstration that IL-13–induced SAPs were dependent on epithelial secretory cell intrinsic IL-4Rα signaling suggests that IL-13 is acting through the type II IL-4R (IL-4Rα/IL-13Rα1).[36] Notably, both IL-4 and IL-13 can signal through the type II IL-4R (IL-4Rα/IL-13Rα1).[37,38] WT BALB/c mice received rmIL-4 (65 ng/200 μL administered intravenously), and 24 hours later, we examined evidence of SI SAPs to test whether IL-4 is sufficient to drive SAPs. We show that exposure of rmIL-4 was sufficient to significantly upregulate MHC class II expression on B cells, confirming IL-4 biological activity (see Fig E3 in this article's Online Repository at www.jacionline.org); however, IL-4 treatment was not sufficient to upregulate the frequency of SI antigen passages (see Fig E3), revealing that SAP formation is an IL-13–specific effect.

BALB/c mice that had previously demonstrated a history of reactivity to foods (fifth challenge) received repeated administration of anti–IL-13Rα1 mAb (Fig 5, *F*) during the sixth and seventh oral OVA challenges and evidence of a food-induced anaphylactic reaction, and SI SAPs were examined to determine the requirement of IL-13–driven SAPs in induction of a food-induced anaphylactic reaction. We show that administration of an anti–IL-13Rα1 mAb to mice with food allergy abrogated MUC2^{+} GCs (Fig 5, *G*) and reduced the frequency of SI SAPs (Fig 5, *G*) compared with isotype control–treated mice. Notably, the reduced frequency of SI SAPs was associated with a significant reduction FIA symptoms (shock and diarrhea; Fig 5, *H*), and this was associated with reduced levels of MC activation (Fig 5, *H*). Spearman rank coefficient correlation analysis revealed a significant negative correlation between the frequency of SAPs and the shock response (Δ temperature change: $r = -0.9649$, $P < .005$), indicating a relationship between SAPs and the severity of oral antigen–induced anaphylaxis. Collectively, these studies indicate that IL-13–induced SI SAPs play a significant role in passage of luminal food allergens across the SI epithelium and severity of oral antigen–induced anaphylaxis.

Pharmacologic blockade of IL-13/CD38-cADPR–driven SAP formation protects mice from the onset of food-induced anaphylactic shock

BALB/c mice that had previously demonstrated a history of reactivity to foods were administered CCh/M4AchR inhibitor (tropicamide) or IL-13/CD38-cADPR inhibitor (8-Br-cADPR) and challenged with OVA to determine the requirement of IL-13/CD38-cADPR-pathway driven SAPs in induction of a food-induced anaphylactic reaction (Fig 6, *A*). Tropicamide treatment did not affect villus SAP formation or food antigen passage in allergic mice or Rh-Dex^{+} MC numbers (Fig 6, *B-D*, and see Videos E3 and E4 in this article's Online Repository at www.jacionline.org), and the mice proceeded to have FIA, as evidenced by hypovolemic shock and MC activation (Fig 6, *E* and *F*). In contrast, pretreating mice with food allergy with 8-Br-cAPDR significantly decreased villus SAP formation and Rh-Dex^{+} MCs (Fig 6, *B-D*) and abrogated MC activation and onset of food-induced anaphylactic symptoms (Fig 6, *E* and *F*, and see Videos E3 and E5 in this article's Online Repository at www.jacionline.org). 8-Br-cADPR or tropicamide treatment did not significantly affect MC degranulation capacity as MC activation induced by EM95 (anti-IgE antibody) treatment and shock response (Fig 6, *G*). Furthermore, 8-Br-cADPR or tropicamide treatment did not affect vascular endothelial function as histamine-induced shock response in 8-Br-cADPR or tropicamide-treated mice was equivalent to that observed in control-treated animals (data not shown). These data indicate that the loss of symptoms of FIA was not a result of 8-Br-cADPR–mediated inhibition of downstream MC activity or histamine-driven shock response.

IL-13–driven SAP formation through the PI3K-CD38-cADPR pathway is conserved in human intestine

To determine whether IL-13–induced SAPs were conserved in human SI, we examined for the presence of SI SAPs in HIOs generated from pluripotent stem cells[26] that were transplanted onto the mesenteries of NSG mice (tHIOs; Fig 7, *A*). Intestinal secretory cells in tHIOs are morphologically and functionally mature and resemble SI epithelium (Fig 7, *B*). Intraluminal administration of fluorescently labeled milk and/or Rd-Dex to the tHIOs of CCh-treated mice revealed the formation of transepithelial food antigen columns in tHIOs (Fig 7, *C*, white arrows, left panel). Notably, milk colocalized with Rh-Dex and was restricted to MUC2^{+} cells and sensitive to M4AchR inhibition, supporting the concept of CCh-dependent GC-restricted antigen passages at steady state (Fig 7, *C*, *E*, and *F*). Administration of IL-13 to tHIOs induced both MUC2^{+}Rh-Dex^{+} and MUC2^{-}Rh-

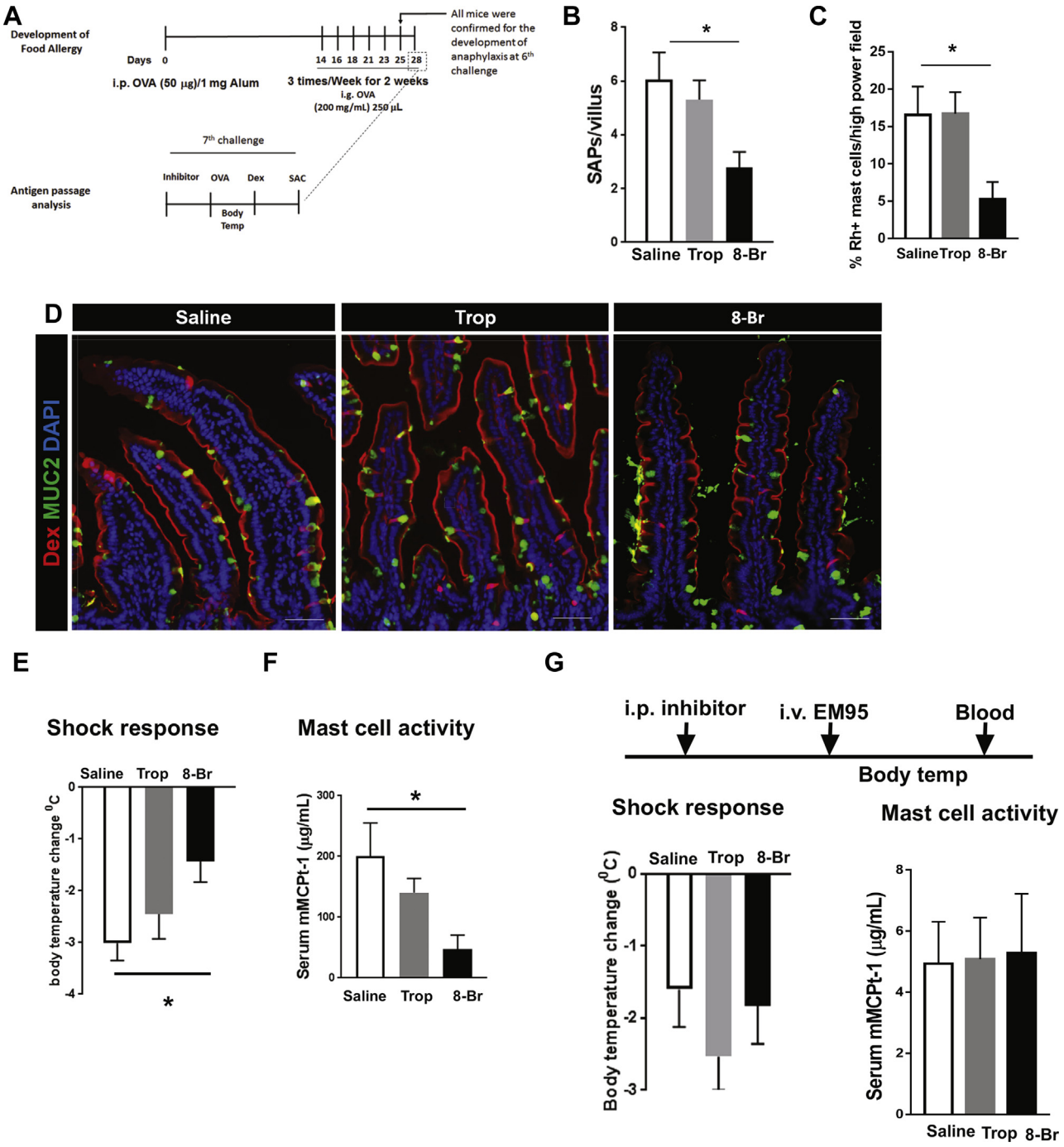

FIG 6. Blocking IL-13–driven SAP formation protects mice from onset of acute food-driven anaphylactic shock. **A,** Diagram depicting experimental design for development of food allergy and analyzing SAP formation during anaphylactic shock in mice. *SAC*, Death followed by tissue harvest. **B,** Quantitation of SAP formation in longitudinal SI sections of mice with food allergy treated with vehicle (saline), tropicamide *(Trop)*, or 8-Br-cADPR *(8-Br)*. **C,** Quantitation of MCs colocalizing with dextran in SI sections of mice with food allergy treated with vehicle (saline), tropicamide *(Trop)*, or 8-Br-cADPR *(8-Br)*. **D,** Immunofluorescence analysis for MUC2 (green) and the nucleus (blue) in cross-sections of SI from allergic mice exposed to Rh-Dex after oral antigen OVA challenge. **E,** Core body temperature measurement in mice after the seventh oral antigen challenge on day 28 that were treated with the indicated inhibitors. **F,** Serum MCPT-1 level analysis in mice treated with the indicated inhibitors. **G,** Experimental design to test the effect of inhibitors on shock response driven by IgE-mediated MC activation. For the shock response, core body temperature was taken after injection of EM95 (anti-IgE antibody), as described with mice treated as indicated. *Mast cell activity*, Serum MCPT-1 levels of mice treated as indicated after injection of EM95. **P* < .05, 1-way ANOVA (n = 3-4 mice per group). *Scale bars* = 50 μm. Data are presented as means ± SEMs. *i.g.*, Intragastric; *i.p.*, intraperitoneal; *i.v.*, intravenous.

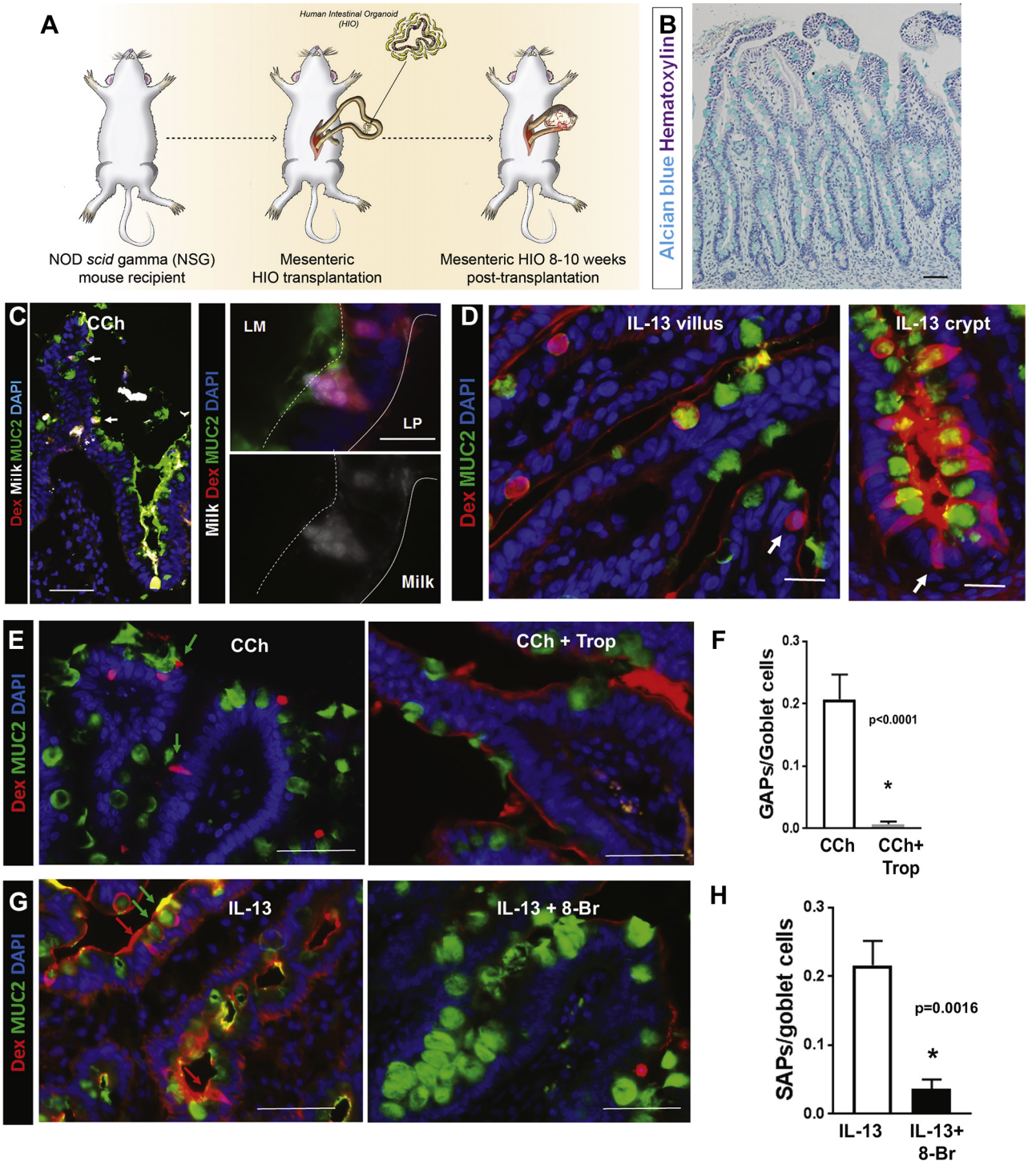

FIG 7. SAP formation pathways are conserved in human intestinal organoids. **A,** Diagram of tHIO generation. **B,** Alcian blue and hematoxylin of a tHIO generated as indicated in Fig 7, *A*. **C,** Immunofluorescence analysis for MUC2 (green) in cross-sections of tHIOs exposed to milk conjugated to Alexa Fluor 647 and Rh-Dex and then stimulated with CCh. Nuclei were visualized with DAPI (blue). *White arrows* indicate $MUC2^{+}$Rho-Dex^{+} milk-negative Alexa Fluor 647^{+} GAPs. Lower-magnification *(left)* and higher-magnification *(right)* images are shown. **D,** Immunofluorescence analysis for MUC2 (green) with cross-sections of tHIOs exposed to Rh-Dex and then stimulated with IL-13. *White arrows* indicate $MUC2^{-}$ antigen passages in villi and crypts. **E** and **F,** Immunofluorescence analysis for MUC2 (green) and nucleus (blue) of tHIOs exposed to Rh-Dex and treated as indicated. *Scale bars* = 50 μm. *Green arrows* indicate $MUC2^{+}$Rho-Dex^{+} antigen passages, and *red arrows* indicate $MUC2^{-}$Rho-Dex^{+} antigen passages. **G** and **H,** Quantification of GAPs (Fig 7, *F*) or SAPs (Fig 7, *H*) in tHIOs (n = 3-4 per group). Student *t* tests were used to determine significance, which was denoted by an *asterisk*.

Dex^+ phenotypes (Fig 7, *D*, white arrows) in the villi and crypts of tHIOs, which was abrogated by 8-Br-cADPR treatment, indicating that IL-13–induced SAP formation in both the villi and crypts is conserved in human intestinal organoids (Fig 7, *G*, red and green arrows, and Fig 7, *H*). These studies reveal that IL-13/CD38/cADPR–dependent SAPs are conserved within human intestinal tissue.

DISCUSSION

Here we demonstrate that food allergens in the SI of mice with food allergy are channeled across the intestinal epithelium through secretory intestinal epithelial cells, which we have termed SAPs. We show that SAP formation and food allergen passage are rapidly induced by food allergens and permit the passage of food allergens to underlying mucosal MCs. We show that the pro–type 2 cytokine IL-13 induces SAPs through a STAT6-independent and CD38-cADPR–sensitive pathway and requires SI intestinal epithelial expression of IL-4Rα. Blockade of this process abrogated food allergen passage across the SI epithelium and diminished induction of a food-induced allergic reaction in mice. Finally, we show that antigen passages and IL-13–induced CD38-cADPR–sensitive SAPs are conserved in human tissue.

Previous studies have revealed that SI steady-state antigen passages are restricted to the SI villus and GCs, primarily driven by an acetylcholine (Ach) muscarinic M4-type receptor (M4AchR)–dependent manner,[31] and unresponsive to commensal microbes but sensitive to epidermal growth factor–mediated inhibition.[31] We show that in mice with food allergy, the luminal antigen-sampling epithelial repertoire in the SI is altered, consisting of additional SI secretory epithelial populations, including enteroendocrine and Paneth cells, and is unresponsive to M4AchR-dependent signaling and dependent on IL-13–induced CD38/cADPR signaling. The participation of additional secretory intestinal epithelial cells in antigen passage during food-induced allergic conditions can be explained by activation through allergic inflammatory pathways, such as IL-13. However, the observation of GC participation in antigen passaging at steady state and during allergic conditions and a shift from an M4AchR-induced to an IL-13–induced M4AchR-unresponsive phenotype suggests a more complex mechanism for GCs. It is possible that GCs involved in antigen passage at steady state are modified by IL-13 and become unresponsive to M4AchR-dependent signaling. Alternatively, different GC subsets might contribute to M4AchR-induced steady state versus IL-13–induced allergic antigen passages. We have previously reported that not all GCs are involved in steady-state antigen passages,[18] and therefore it is possible that different GC subsets are involved in antigen passage during the allergic condition versus those involved in antigen passage at steady state. Differential involvement of GC subsets in antigen passage formation at steady state and under allergic conditions might explain the differential interactions with hematopoietic cells, such as dendritic cells and MCs.

Our data support the concept that the alteration in antigen-sampling epithelial repertoire in the SI of mice with food allergy is directly mediated by IL-13. We showed that (1) ectopic transgenic expression of IL-13 in the SI was sufficient to drive SAP formation, (2) that SAP formation required intestinal secretory cell IL-4Rα expression, and (3) that administration of hIL-13 to NSG mice (which lack the adaptive immune cells) was sufficient to induce SAPs in tHIOs. IL-13 has previously been reported to stimulate GC hyperplasia and mucus secretion, Paneth cell degranulation, and entoerendocrine cell function.[39-41] The present study identifies a novel role for IL-13 in regulation of intestinal secretory epithelial cell function associated with food antigen translocation and induction of food-induced allergic reactions. The cellular source of IL-13 for SAP induction in the SIs of mice with food allergy is currently not fully delineated. Group 2 innate lymphoid cells (ILC2s) might be the cellular source of IL-13 as ILC2s are a major source of IL-13 in food-allergic mice and have been shown to be required for the onset of food allergy.[32]

We have previously demonstrated that genetic or pharmacologic deletion of GAPs was associated with a loss of antigen delivery to SI lamina propria dendritic cells, suggesting that SI GAPs are the primary pathway for delivery of SI luminal antigen to the adaptive immune compartment in the basal state.[18] In the present study we show that SAPs facilitate food allergen passage to SI MCs, indicating that multiple hematopoietic cell populations can acquire antigen through intestinal epithelial passages. Fluorescent microscopic analysis revealed that in mice with food allergy, mucosal MCs appear to predominantly localize to the basolateral membranes of SAPs. Demonstration that food antigen exposure led to rapid channeling of antigen through the SAPs and acquisition by MCs immediately beneath the lateral membrane of the SAPs makes it tempting to speculate that MCs are selectively recruited to this location to sense luminal antigens channeled by SAPs.[42] This might explain the concentrated amplification of mucosal MCs within the subepithelial region that is dependent on IL-9–driven SI mastocytosis required in induction of food-induced reactions in mice.[25]

In vitro analyses revealed that IL-13 stimulation of LS174T cells led to heightened $[Ca^{2+}]_i$ responses and antigen passages that were STAT6 independent and inhibited by 8-Br-cADPR. Previous studies have reported that IL-13 stimulation of human airway smooth muscle cells leads to increased CD38 expression and ADP-ribosyl cyclase activity, which was associated with heightened $[Ca^{2+}]_i$ activity and responsive to 8-Br-cADPR.[34,43] IL-13 activation of the type II IL-4R pathway (IL-4Rα–IL-13Rα1) leads to IL-4Rα–bound insulin receptor substrate 2 (IRS-2) phosphorylation and activation of the PI3K-Akt pathway stimulating $[Ca^{2+}]_i$ activity.[36,44] Collectively, these studies establish a link between GC secretion by compound exocytosis, $[Ca^{2+}]_i$ activity, and SAP formation.

The precise mechanism by which food allergens stimulate SAP formation and passage of antigens to mucosal MCs is currently unknown. We demonstrate that mice with food allergy have SAPs and that food allergen exposure rapidly enhances SAP formation. Berin et al[45] have previously reported that oral antigen exposure of rat SI led to rapid antigen uptake into vesicles of epithelial cells of the SI. SI epithelial antigen uptake was linked to expression of the low-affinity IgE receptor (FcεRII) on SI intestinal epithelial cells, and neutralization of FcεRII function inhibited luminal antigen uptake.[46] It is not clear whether FcεRII or IgE is involved in SAP formation and antigen translocation. However, given that administration of hIL-13 to NSG mice is sufficient to stimulate SAPs in tHIOs suggests that additional mechanisms beyond adaptive immune recognition pathways are involved in the process.

Previously, we have reported that GAPs within the gastrointestinal tract channel luminal high-molecular-weight substances

to lamina propria antigen-presenting cells, such as $CD11c^+$ dendritic cells, and drive antigen-specific T-cell responses.[18,47] These studies raise the concept that GCs and GAPs can contribute to delivery of luminal food antigens to the immune compartment for induction of T-cell responses outside of the organized lymphoid tissues and regulate oral tolerance versus food sensitization. The role of GAPs in inducing tolerance to dietary antigens at steady state is yet to be explored. However, experimental evidence demonstrating that dysregulation of GAP activity promotes inflammatory T-cell responses to dietary antigens[48] and our observations that certain conditions, such as increased levels of type 2 cytokines, can alter SI epithelial antigen passage patterning (GAPs vs SAPs) and promote channeling of antigens to additional cell populations, such as MCs, leads one to speculate that dysregulation of antigen passage might lead to altered responsiveness to dietary antigens (oral tolerance vs food sensitization). Consistent with this concept, modulation of GAP patterning of the gastrointestinal tract during the preweaning stage in mice can alter susceptibility to colitis.[49]

In summary, we identify SI SAPs in mice with food allergy, and that these processes are enhanced by allergen exposure to rapidly channel food allergens across the SI epithelium. We show that both mouse and human SI SAPs are induced by IL-13 in a CD38/cADPR-dependent manner and are required for passage of food allergens across the SI epithelium and induction of a food-induced anaphylactic reaction. These studies reveal the ability of the proallergic cytokine IL-13 to remodel the SI antigen uptake architecture under conditions of food allergy, which enables routing of luminal antigens to intestinal MCs and induction of food-induced anaphylactic reactions. Given that T_H2 cytokine responses are associated with other afflictions (eg, helminthic infestation) and allergic diseases (eg, allergic rhinitis and asthma), SAPs can extend to other T_H2-driven conditions. Indeed, SAPs might be a generalizable hallmark of IL-13–induced immune responses at the mucosal surfaces, and strategies to circumvent SAPs might have therapeutic potential for many T_H2-associated conditions.

We thank members of the Division of Allergy and Immunology and Dr Fred Finkelman at CCHMC for critical review of the manuscript and insightful conversations. We also thank Shawna Hottinger for editorial assistance and manuscript preparation.

Key messages

- **The processes by which food allergens cross the mucosal surface and are delivered to the subepithelial immune compartment to promote the clinical manifestations of FIA are largely unexplored.**
- **Food allergens are sampled by SI epithelial secretory cells (termed SAPs) that are localized to the SI villus and crypt region.**
- **SAPs channel food allergens to lamina propria mucosal MCs through a IL-13–CD38–cADPR–dependent process, and blockade of this process inhibited induction of clinical manifestations of FIA.**
- **IL-13–induced SAP sampling of food allergens was conserved in HIOs.**

REFERENCES

1. Sicherer SH, Sampson HA. Food allergy: epidemiology, pathogenesis, diagnosis, and treatment. J Allergy Clin Immunol 2014;133:291-308.
2. Motosue MS, Bellolio MF, Van Houten HK, Shah ND, Campbell RL. Increasing emergency department visits for anaphylaxis, 2005-2014. J Allergy Clin Immunol Pract 2017;5:171-5.e3.
3. Galli SJ, Kalesnikoff J, Grimbaldeston MA, Piliponsky AM, Williams CMM, Tsai M. Mast cells as "tunable" effector and immunoregulatory cells: recent advances. Annu Rev Immunol 2005;23:749-86.
4. Strait RT, Morris SC, Yang M, Qu XW, Finkelman FD. Pathways of anaphylaxis in the mouse. J Allergy Clin Immunol 2002;109:658-68.
5. Dombrowicz D, Flamand V, Brigman KK, Koller BH, Kinet JP. Abolition of anaphylaxis by targeted disruption of the high affinity immunoglobulin E receptor alpha chain gene. Cell 1993;75:969-76.
6. Lorentz A, Schwengberg S, Mierke C, Manns MP, Bischoff SC. Human intestinal mast cells produce IL-5 in vitro upon IgE receptor cross-linking and in vivo in the course of intestinal inflammatory disease. Eur J Immunol 1999;29:1496-503.
7. Santos J, Benjamin M, Yang PC, Prior T, Perdue MH. Chronic stress impairs rat growth and jejunal epithelial barrier function: role of mast cells. Am J Physiol Gastrointest Liver Physiol 2000;278:G847-54.
8. Kelefiotis D, Vakirtzi-Lemonias C. In vivo responses of mouse blood cells to platelet-activating factor (PAF): role of the mediators of anaphylaxis. Agents Actions 1993;40:150-6.
9. Strait RT, Morris SC, Smiley K, Urban JF Jr, Finkelman FD. IL-4 exacerbates anaphylaxis. J Immunol 2003;170:3835-42.
10. Sampson HA. Food allergy. Part 2: diagnosis and management. J Allergy Clin Immunol 1999;103:981-9.
11. Sampson HA. Food allergy. Part 1: immunopathogenesis and clinical disorders. J Allergy Clin Immunol 1999;103:717-28.
12. Wang J, Sampson HA. Food allergy. J Clin Invest 2011;121:827-35.
13. Galli SJ, Tsai M. IgE and mast cells in allergic disease. Nat Med 2012;18:693-704.
14. Hase K, Kawano K, Nochi T, Pontes GS, Fukuda S, Ebisawa M, et al. Uptake through glycoprotein 2 of FimH(+) bacteria by M cells initiates mucosal immune response. Nature 2009;462:226-30.
15. Neutra MR. M cells in antigen sampling in mucosal tissues. Curr Top Microbiol Immunol 1999;236:17-32.
16. Neutra MR, Frey A, Kraehenbuhl JP. Epithelial M cells: gateways for mucosal infection and immunization. Cell 1996;86:345-8.
17. Rescigno M, Urbano M, Valzasina B, Francolini M, Rotta G, Boasio R, et al. Dendritic cells express tight junction proteins and penetrate gut epithelial monolayers to sample bacteria. Nat Immunol 2001;2:361-7.
18. McDole JR, Wheeler LW, McDonald KG, Wang B, Konjufca V, Knoop KA, et al. Goblet cells deliver luminal antigen to CD103+ dendritic cells in the small intestine. Nature 2012;483:345-9.
19. Turner JR. Intestinal mucosal barrier function in health and disease. Nat Rev Immunol 2009;9:799-809.
20. Wu D, Ahrens R, Osterfeld H, Noah TK, Groschwitz K, Foster PS, et al. Interleukin-13 (IL-13)/IL-13 receptor alpha1 (IL-13Ralpha1) signaling regulates intestinal epithelial cystic fibrosis transmembrane conductance regulator channel-dependent Cl-secretion. J Biol Chem 2011;286:13357-69.
21. Lo YH, Chung E, Li Z, Wan YW, Mahe MM, Chen MS, et al. Transcriptional regulation by ATOH1 and its target SPDEF in the intestine. Cell Mol Gastroenterol Hepatol 2017;3:51-71.
22. Ahrens R, Osterfeld H, Wu D, Chen CY, Arumugam M, Groschwitz K, et al. Intestinal mast cell levels control severity of oral antigen-induced anaphylaxis in mice. Am J Pathol 2012;180:1535-46.
23. Rose MF, Ahmad KA, Thaller C, Zoghbi HY. Excitatory neurons of the proprioceptive, interoceptive, and arousal hindbrain networks share a developmental requirement for Math1. Proc Natl Acad Sci U S A 2009;106:22462-7.
24. Herbert DR, Holscher C, Mohrs M, Arendse B, Schwegmann A, Radwanska M, et al. Alternative macrophage activation is essential for survival during schistosomiasis and downmodulates T helper 1 responses and immunopathology. Immunity 2004;20:623-35.
25. Forbes EE, Groschwitz K, Abonia JP, Brandt EB, Cohen E, Blanchard C, et al. IL-9- and mast cell-mediated intestinal permeability predisposes to oral antigen hypersensitivity. J Exp Med 2008;205:897-913.
26. Watson CL, Mahe MM, Munera J, Howell JC, Sundaram N, Poling HM, et al. An in vivo model of human small intestine using pluripotent stem cells. Nat Med 2014;20:1310-4.
27. Yamani A, Wu D, Waggoner L, Noah T, Koleske AJ, Finkelman F, et al. The vascular endothelial specific IL-4 receptor alpha-ABL1 kinase signaling axis

regulates the severity of IgE-mediated anaphylactic reactions. J Allergy Clin Immunol 2018;142:1159-75.e5.
28. Chen CY, Lee JB, Liu B, Ohta S, Wang PY, Kartashov A, et al. Induction of interleukin-9-producing mucosal mast cells promotes susceptibility to IgE-mediated experimental food allergy. Immunity 2015;43:788-802.
29. Noah TK, Kazanjian A, Whitsett J, Shroyer NF. SAM pointed domain ETS factor (SPDEF) regulates terminal differentiation and maturation of intestinal goblet cells. Exp Cell Res 2010;316:452-65.
30. Osterfeld H, Ahrens R, Strait R, Finkelman FD, Renauld JC, Hogan SP. Differential roles for the IL-9/IL-9 receptor alpha-chain pathway in systemic and oral antigen-induced anaphylaxis. J Allergy Clin Immunol 2010;125:469-76.e2.
31. Knoop KA, McDonald KG, McCrate S, McDole JR, Newberry RD. Microbial sensing by goblet cells controls immune surveillance of luminal antigens in the colon. Mucosal Immunol 2015;8:198-210.
32. Lee JB, Chen CY, Liu B, Mugge L, Angkasekwinai P, Facchinetti V, et al. IL-25 and CD4(+) TH2 cells enhance type 2 innate lymphoid cell-derived IL-13 production, which promotes IgE-mediated experimental food allergy. J Allergy Clin Immunol 2016;137:1216-25.e5.
33. Shroyer NF, Helmrath MA, Wang VY, Antalffy B, Henning SJ, Zoghbi HY. Intestine-specific ablation of mouse atonal homolog 1 (Math1) reveals a role in cellular homeostasis. Gastroenterology 2007;132:2478-88.
34. Deshpande DA, Dogan S, Walseth TF, Miller SM, Amrani Y, Panettieri RA, et al. Modulation of calcium signaling by interleukin-13 in human airway smooth muscle: role of CD38/cyclic adenosine diphosphate ribose pathway. Am J Respir Cell Mol Biol 2004;31:36-42.
35. Birchenough GM, Johansson ME, Gustafsson JK, Bergstrom JH, Hansson GC. New developments in goblet cell mucus secretion and function. Mucosal Immunol 2015;8:712-9.
36. Wills-Karp M, Finkelman FD. Untangling the complex web of IL-4- and IL-13-mediated signaling pathways. Sci Signal 2008;1:pe55.
37. Nelms K, Keegan AD, Zamorano J, Ryan JJ, Paul WE. The IL-4 receptor: signaling mechanisms and biologic functions. Annu Rev Immunol 1999;17:701-38.
38. Hershey GK. IL-13 receptors and signaling pathways: an evolving Web. J Allergy Clin Immunol 2003;111:677-90.
39. Kondo M, Tamaoki J, Takeyama K, Nakata J, Nagai A. Interleukin-13 induces goblet cell differentiation in primary cell culture from Guinea pig tracheal epithelium. Am J Respir Cell Mol Biol 2002;27:536-41.
40. Stockinger S, Albers T, Duerr CU, Menard S, Putsep K, Andersson M, et al. Interleukin-13-mediated Paneth cell degranulation and antimicrobial peptide release. J Innate Immun 2014;6:530-41.
41. McDermott JR, Leslie FC, D'Amato M, Thompson DG, Grencis RK, McLaughlin JT. Immune control of food intake: enteroendocrine cells are regulated by CD4+ T lymphocytes during small intestinal inflammation. Gut 2006;55:492-7.
42. Abonia JP, Austen KF, Rollins BJ, Joshi SK, Flavell RA, Kuziel WA, et al. Constitutive homing of mast cell progenitors to the intestine depends on autologous expression of the chemokine receptor CXCR2. Blood 2005;105:4308-13.
43. Deshpande DA, Walseth TF, Panettieri RA, Kannan MS. CD38/cyclic ADP-ribose-mediated Ca2+ signaling contributes to airway smooth muscle hyper-responsiveness. FASEB J 2003;17:452-4.
44. Keegan AD, Nelms K, White M, Wang L, Pierce JH, Paul WE. An IL-4 receptor region containing an insulin receptor motif is important for IL-4 mediated IRS-1 phosphorylation and cell growth. Cell 1994;76:811-20.
45. Berin MC, Kiliaan AJ, Yang PC, Groot JA, Taminiau JA, Perdue MH. Rapid transepithelial antigen transport in rat jejunum: impact of sensitization and the hypersensitivity reaction. Gastroenterology 1997;113:856-64.
46. Yang PC, Berin MC, Yu LC, Conrad DH, Perdue MH. Enhanced intestinal transepithelial antigen transport in allergic rats is mediated by IgE and CD23 (FcεRII). J Clin Invest 2000;106:879-86.
47. Knoop KA, Newberry RD. Goblet cells: multifaceted players in immunity at mucosal surfaces. Mucosal Immunol 2018;11:1551-7.
48. Kulkarni DH, McDonald KG, Knoop KA, Gustafsson JK, Kozlowski KM, Hunstad DA, et al. Goblet cell associated antigen passages are inhibited during *Salmonella typhimurium* infection to prevent pathogen dissemination and limit responses to dietary antigens. Mucosal Immunol 2018;11:1103-13.
49. Knoop KA, Gustafsson JK, McDonald KG, Kulkarni DH, Coughlin PE, McCrate S, et al. Microbial antigen encounter during a preweaning interval is critical for tolerance to gut bacteria. Sci Immunol 2017;2.

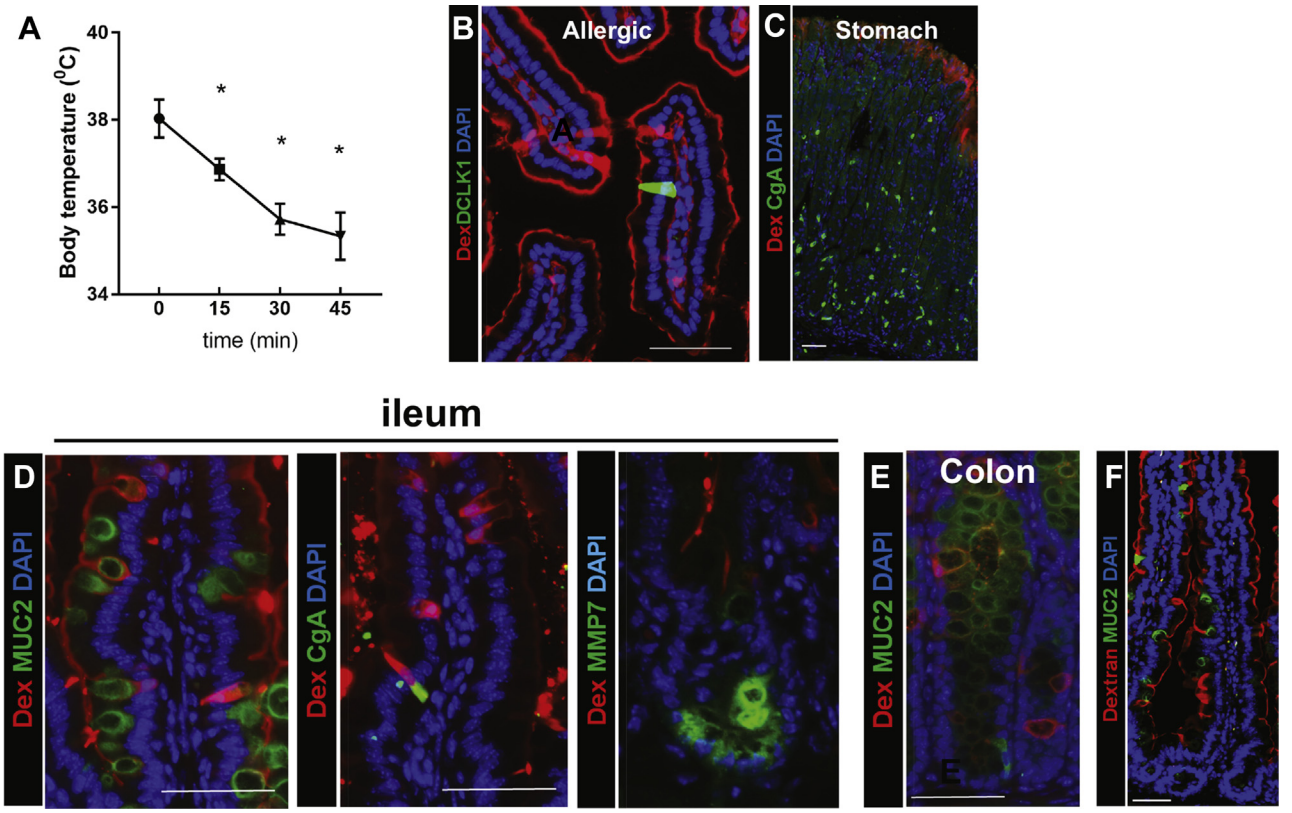

FIG E1. Antigen-positive cells in the gastrointestinal segments of mice with food allergy. **A,** Core body temperature of mice with food allergy after oral allergen challenge (n = 9). Food allergy was induced in BALB/c mice, as depicted in Fig 1, *D*. Core body temperature was measured after the seventh oral allergen challenge at day 28. **P* < .05. **B,** Immunofluorescence analysis for the tuft cell marker DCKL1 in SI from mice with food allergy exposed to Rho-Dex (red). **C-E,** Immunofluorescence analysis for CgA, MUC2, or MMP7 (green) in the stomach (Fig E1, *C*), ileum (Fig E1, *D*), or colon (Fig E1, *E*) of mice with food allergy. Nuclei are visualized with DAPI (blue). **F,** Immunofluorescence analysis for MUC2 in SI of control mice that went through tamoxifen treatment as *Atoh1*-deleted (*Atoh1*-MT) mice and were then exposed to Rho-Dex. *Scale bars* = 50 μm.

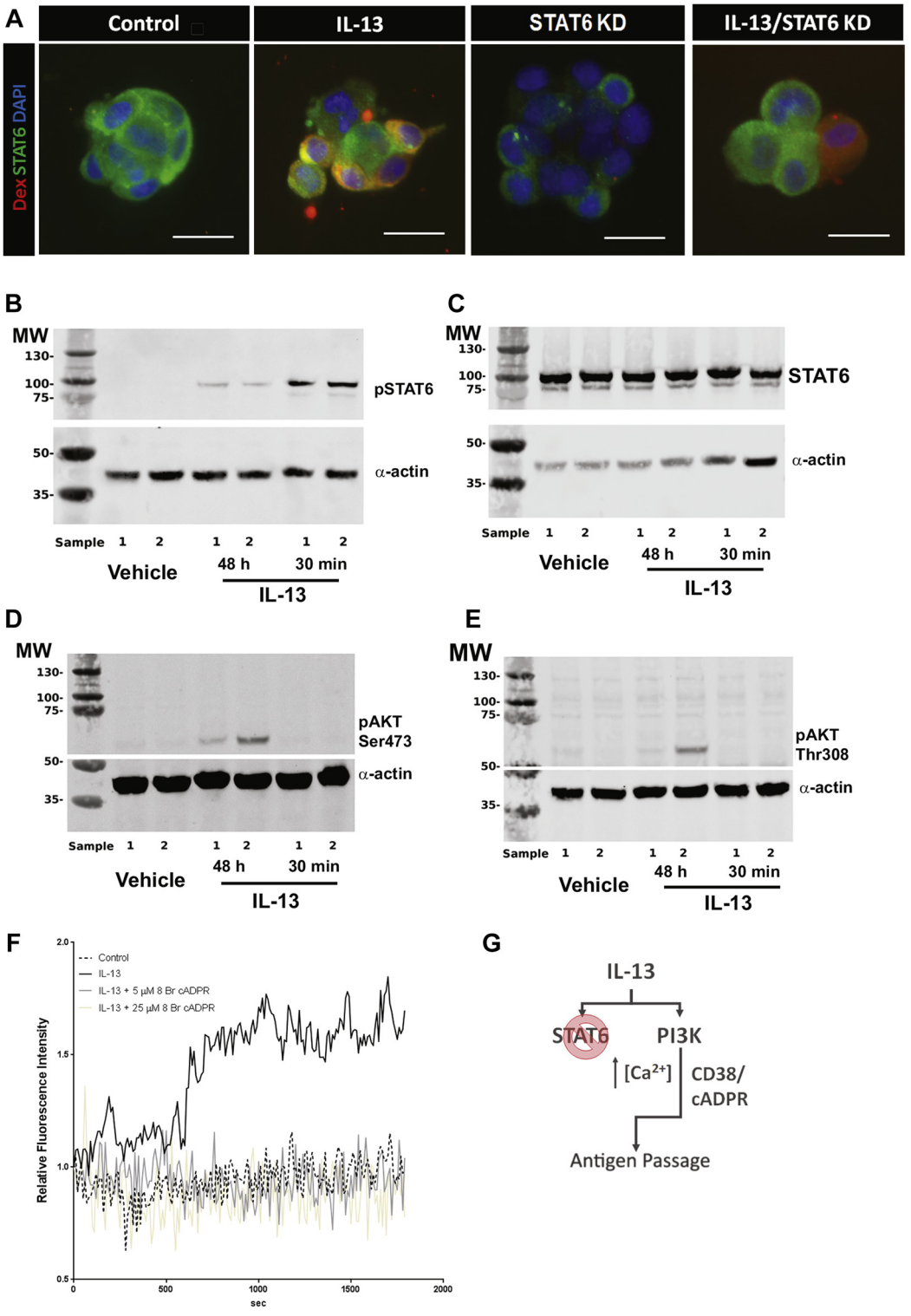

FIG E2. IL-13 induction of antigen passage through a STAT6-independent process. **A,** Immunofluorescence analysis for STAT6 (green) with cells transduced with lentivirus carrying control short hairpin RNA (control and IL-13) or anti-STAT6 short hairpin RNA (STAT6 KD and IL-13/STAT6 KD) to reduce protein expression of STAT6 (green). Cells were stimulated with vehicle (control and STAT6 KD) or IL-13 (IL-13 and IL-13/STAT6 KD) and exposed to Rh-Dex (red) to examine antigen uptake. **B-E,** Western blot analysis for phosphorylated STAT6 (Fig E2, *B*), STAT6 (Fig E2, *C*), phosphorylated AKT (pAKT) Ser 473 (Fig E2, *D*), and phosphorylated AKT Thr 306 (Fig E2, *E*). Cell lysates were collected from cells treated with vehicle or IL-13 for the durations indicated. Actin was used as a loading control. *MW*, Molecular weight. **F,** Graph showing $[Ca^{2+}]_i$ levels in LS174T cells over 30 minutes after treatment as indicated: vehicle (control), IL-13, or IL-13 and cADPR antagonist (8-Br-cADPR at 5 or 25 μmol/L). **G,** Diagram summarizing the pathway involved in IL-13–driven antigen uptake in a mucinous colonic cancer cell line: LS174T cells. *Scale bars* = 50 μm.

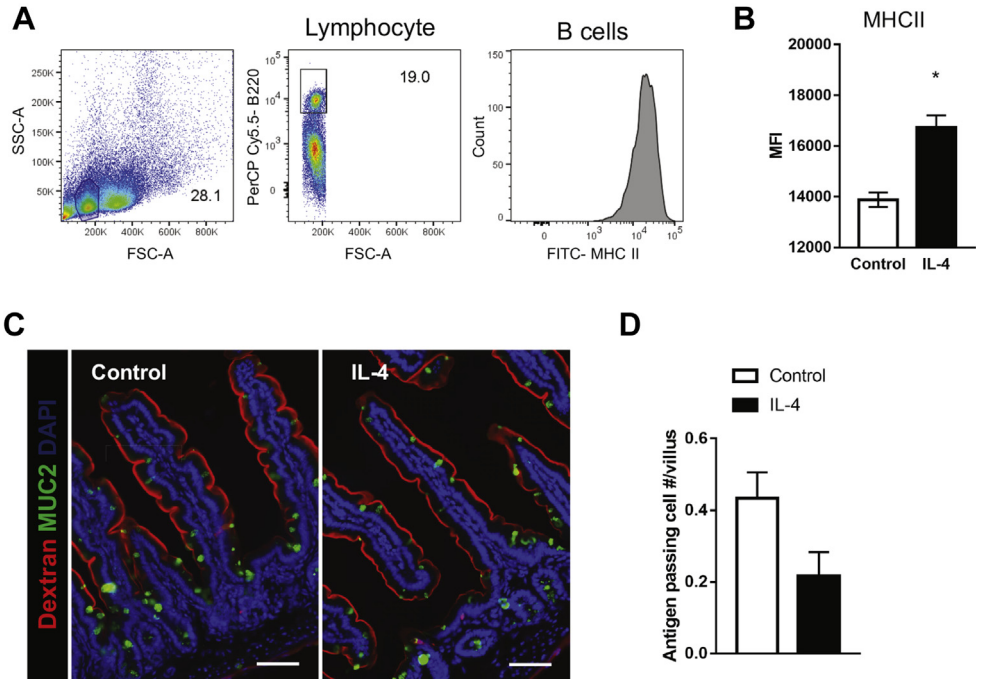

FIG E3. IL-4 does not drive antigen passage formation in the SI. **A,** Flow cytometric analyses indicating gating strategies of splenic B cells ($B220^{+}$) and levels of MHC class II expression. *FSC*, Forward scatter; *SSC*, side scatter. **B,** Mean fluorescence intensity *(MFI)* of MHC class II on $B220^{+}$ splenic B cells from control and IL-4–treated mice. **C,** Immunofluorescence analysis for MUC2 (green) and Rh-Dex (red) in SI from control and IL-4–treated mice. **D,** Quantitation of antigen-passing intestinal epithelial cells per villus in SI from control and IL-4–treated mice. *Scale bars* = 50 μm. The nucleus is visualized with DAPI. *Statistical significance: $P < .05$.